UNIVERSIDADE DE LISBOA
FACULDADE DE CIÊNCIAS
DEPARTAMENTO DE BIOLOGIA VEGETAL

Development of 3D epidermal models: towards the development of a skin model for studies of the autosomal recessive spastic ataxia of Charlevoix-Saguenay (ARSACS)

Maria Beatriz Costa Teixeira

Mestrado em Biologia Molecular e Genética

Dissertação orientada por:

Professor Doutor Abel Oliva
Professor Doutor Federico Herrera

2021

Acknowledgments

Many people have greatly contributed to this work to whom I would like to express my deepest gratitude.

First of all, I would like to thank my supervisors Dr. Abel Oliva and Dr. Federico Herrera for allowing me to conduct my project in their laboratories, for believing in me and for their guidance and great advice.

I would like to thank all the people from the Biomolecular Diagnostic laboratory for the friendly environment and constant support. In particular, I would like to thank Sara and Mafalda for their invaluable help and for everything they taught me. This work would not have been possible without them.

I want to thank everyone from the Cell Structure and Dynamics laboratory for receiving me in their lab and for making me feel welcome. A very special thank you to Fernanda for her fundamental contribution to this work. I appreciate your patience, the time you took to teach me, and our conversations that allowed me to grow as a scientist.

Last but not least, I would like to thank my family and friends for their incredible support and motivation during this period.

Abstract

The skin is a complex organ mainly responsible for protecting the body from external threats and maintaining homeostasis. It is a complex three-dimensional structure that is composed of two main compartments, the dermis and the epidermis. Due to increasing ethical and legal pressure on animal usage in research, reconstructed 3D human skin models have been gaining popularity. These models mimic human skin architecture *in vitro* and allow relatively easy manipulation to meet specific needs. Some rare diseases remain poorly studied and could take advantage of this technology. One example is the Autosomal Recessive Spastic Ataxia of Charlevoix-Saguenay (ARSACS) which is an early-onset neurological disease that was first described in Quebec, Canada, but cases have been reported worldwide. Patients suffer from spasticity and lack of coordination of muscle movements, resulting in an early wheelchair dependence and premature death. ARSACS is caused by loss-of-function mutations in the *SACS* gene, leading to a defective sacsin protein. Sacsin loss of function has been linked to mitochondrial dysfunction and abnormalities in the organization of intermediate filaments, but the complete picture is still unclear. Evidence of abnormalities in the skin of ARSACS patients has been reported, making this disease an interesting candidate to be studied using *in vitro* skin models.

In this work, two different human keratinocyte cell lines (HaCaT and N/TERT-1) were used to create new human epidermal models using a polycarbonate inert matrix. The localization of different keratins and other markers (keratins 10, 14 and 15, and involucrin) were studied to characterize epidermal differentiation and stratification. Sacsin expression was analyzed in different cell lines and sacsin knockdown was attempted in HaCaT keratinocytes using lentiviral shRNAs.

The HaCaT cell line was unable to recreate the normal multi-layer architecture of native skin nor the *stratum corneum*. This cell line expressed low amounts of the sacsin protein, and no difference was observed between the knockdown and the control by western blot. N/TERT-1 keratinocytes generated a stratified epidermis with all the normal layers present, including the *stratum corneum*. Complete epidermal differentiation was confirmed by the differential expression of epidermal markers. K14 expression was limited to the basal layer, while K10 was expressed in the upper layers, as expected. Involucrin was mostly expressed in the *stratum granulosum* and K15 expression was overall very low, indicating a successful differentiation. Sacsin expression was verified in different skin cells (HEKn, HDFn, and N/TERT-1), and N/TERT-1 expressed sacsin in amounts slightly lower than primary human keratinocytes. These findings suggest that the N/TERT-1 cell line has more potential to produce an epidermal skin model with an ARSACS phenotype, which can prove an important tool in future research.

Despite the existing knowledge about sacsin structure and function, a lot is still unknown about this protein and how it causes the symptoms underlying ARSACS disease. Advances in this topic could contribute to the development of therapies that could cure or tackle some of ARSACS symptoms to ensure a better quality of life for the patients.

Keywords: HaCaT, N/TERT-1, Epidermal model, ARSACS, Sacsin

Resumo

A pele é um órgão complexo, responsável principalmente pela proteção do organismo contra ameaças externas e pela manutenção da homeostase. É uma estrutura tridimensional que é composta por dois compartimentos principais, a derme e a epiderme. Devido à crescente pressão ética e legal sobre a utilização de animais para fins de investigação, clínicos e industriais e a proibição na União Europeia de ensaios em animais de produtos cosméticos e ingredientes ativos para uso cosmético, os modelos tridimensionais de pele humana *in vitro* têm vindo a ganhar uma popularidade crescente. Quando comparados com culturas celulares bidimensionais, os modelos tridimensionais são capazes de recapitular melhor a fisiologia *in vivo*, permitindo interações entre as células e entre estas e a matriz extracelular que mimetizam a morfologia da pele humana, permitindo também uma fácil manipulação para usos específicos. Um dos fatores mais importantes a ter em consideração nestes modelos é o tipo de células utilizadas, que podem ser células primárias ou linhas celulares. As células primárias humanas são isoladas de procedimentos cirúrgicos em pacientes voluntários, sendo o tipo de células mais comum devido ao facto de possuírem uma melhor capacidade de diferenciação. No entanto, as células primárias apresentam algumas desvantagens, não só devido à variação dos dadores, mas também devido à sua restrita capacidade de proliferação. Estes problemas podem ser colmatados com a utilização de linhas celulares imortalizadas.

Algumas doenças raras continuam a ser pouco estudadas e poderiam tirar partido desta tecnologia. Um exemplo é a Ataxia espástica de Charlevoix-Saguenay (*Autosomal Recessive Spastic Ataxia of Charlevoix-Saguenay* - ARSACS), que é uma doença neurológica precoce que foi descrita pela primeira vez na região de Québec no Canadá, mas vários casos já foram descritos em vários países. Os pacientes sofrem de espasticidade e falta de coordenação dos movimentos musculares, resultando numa dependência precoce da cadeira de rodas e em morte prematura. ARSACS é causado pelas mutações no gene *SACS*, levando à produção de uma proteína *sacsin* defetuosa. Esta proteína possui um elevado peso molecular (520 kDa) e a sua arquitetura sugere que possa funcionar como co-chaperone. A perda de função desta proteína foi associada a disfunções mitocondriais e anomalias na organização dos filamentos intermédios, mas ainda existem várias questões por responder. Foram relatadas evidências de anomalias cutâneas nos pacientes com ARSACS, tornando esta doença um tema de interesse para estudar recorrendo a modelos de pele *in vitro*.

Tirando partido da tecnologia de modelos de pele *in vitro*, um dos objetivos deste projeto é desenvolver e caracterizar novos modelos de epiderme tridimensionais utilizando queratinócitos imortalizados provenientes de linhas celulares. Por outro lado, pretende-se explorar o papel da proteína *sacsin* nas células da pele, a fim de determinar se é possível desenvolver um modelo de pele que apresente o fenótipo de ARSACS. Neste trabalho, foram utilizadas duas linhas celulares de queratinócitos humanos (HaCaT e N/TERT-1) para criar novos modelos de epiderme tridimensionais utilizando uma matriz de policarbonato comercial. Os queratinócitos foram semeados nesta matriz, na qual ficaram submersos por meio de cultura durante um período que variou para cada linha celular (para a linha celular HaCaT o período foi de 24h, enquanto que para a linha N/TERT-1 foi de 72h). Posteriormente, as culturas celulares foram submetidas a condições de interface ar-líquido (*air-liquid interface*- ALI), que consistiu na remoção completa do meio da parte superior das culturas. A localização de diferentes queratinas e outros marcadores da epiderme (queratinas 10, 14, 15 e involucrina) foram estudados nos modelos desenvolvidos através de imunoflorescência, de modo a avaliar a diferenciação e estratificação da epiderme. Foram também realizados estudos da expressão da proteína *sacsin* em diferentes linhas celulares, bem como tentativas no sentido de eliminar a sua expressão (*sacsin knockdown*) em queratinócitos HaCaT utilizando shRNAs lentivirais.

Em primeiro lugar estudámos como diferentes condições de cultura celular afetaram o desenvolvimento do modelo de epiderme utilizando células HaCaT. Foram testadas duas composições de meios, Epilife e DMEM, testando-se a suplementação de diferentes concentrações de cálcio nas diferentes fases do desenvolvimento da epiderme com o meio Epilife. A diferenciação da epiderme não foi observada quando o meio DMEM foi utilizado, sugerindo que provavelmente a suplementação de FBS ou a concentração de cálcio pode ter inibido a estratificação desta linha celular. Apesar do modelo de epiderme com HaCaT desenvolvido neste trabalho ter apresentado algum grau de estratificação, os estratos presentes na normal morfologia da epiderme humana não foram observados. Com o aumento do número de dias em condições de ALI, duas camadas tornam-se mais evidentes no modelo de epiderme: uma camada basal que se assemelha ao *stratum basale* da epiderme nativa e uma camada superior onde as células apresentavam um arranjo desorganizado e mais disperso. Apesar de se ter observado um aumento na espessura da epiderme à medida que o número de dias em condições ALI aumentava, não houve formação de *stratum corneum* mesmo após 31 dias em condições ALI. A morfologia deste modelo partilhava algumas características de epitélios pseudoqueratinizados (*parakeratotic epithelia*), como a presença de núcleos nas camadas mais exteriores devido à diferenciação incompleta dos queratinócitos.

Em relação á linha N-TERT-1, de modo a promover a adesão celular à matriz de policarbonato, foi necessário fazer o revestimento com colagénio tipo I antes de semear os queratinócitos. Foi possível observar os diferentes estratos característicos de uma epiderme totalmente diferenciada: O *stratum basale*, no qual as células apresentavam uma forma cuboidal, com um arranjo compacto e altamente proliferativas, o *stratum spinosum* onde as células apresentavam uma forma mais alongada, e acima o *stratum granulosum*, caracterizado pelo aparecimento de grânulos no interior das células. Ao contrário do que foi observado no modelo com células HaCaT, neste caso foi possível observar a formação do *stratum corneum*, a última fase do processo de maturação da epiderme.

A maturação progressiva dos queratinócitos que se inicia no *stratum basale* e termina no *startum corneum*, onde atingem diferenciação terminal, é acompanhada pela expressão de diferentes proteínas, entre estas as queratinas. A expressão de queratina 14 (K14) no modelo HaCaT foi superior na camada basal da epiderme apesar de também ser visível nas camadas superiores. No modelo N/TERT-1, a expressão de K14 estava restrita à camada basal da epiderme, o que está de acordo com o descrito para a epiderme humana. A K10 foi expressa em ambos os modelos nas camadas superiores da epiderme, mas não na camada basal. A expressão de involucrina, que é juntamente com a K10 outro marcador de diferenciação, foi reduzida no modelo HaCaT e no modelo N/TERT-1 estava principalmente localizada no *stratum granulosum*. A expressão da K15 na epiderme está associada a um fenótipo indiferenciado, pelo que a sua expressão no modelo HaCaT ao longo das camadas da epiderme pode ser outro indicador de que os queratinócitos HaCaT não atingiram um estado de completa diferenciação. As epidermes produzidas pelas células N/TERT-1 não expressaram este marcador, o que é consistente com uma epiderme mais desenvolvida e com maior grau de diferenciação.

A expressão de *sacsin* foi estudada em múltiplas células cutâneas: HaCaT, N/TERT-1, queratinócitos primários (HEK) e fibroblastos primários (HDFn). As células HaCaT expressaram níveis baixos de *sacsin* quando comparadas com as células C6 de glioma de ratinho (controlo positivo para expressão de *sacsin*). Utilizou-se a tecnologia de RNA (shRNA) através de transdução lentiviral de modo a depletar a expressão de *sacsin* nas células HaCaT, mas a expressão da *sacsin* não foi observada nem nas células HaCaT que foram transduzidas, nem controlo não transduzido. A ausência da expressão de *sacsin* no grupo das HaCaT controlo não permitiu concluir se a ausência de *sacsin* no grupo tratado com shRNA foi resultado da experiência ou simplesmente devido ao facto de a expressão desta proteína ser muito baixa na subpopulação de HaCaT utilizada nesta experiência.

Para caracterizar a expressão de *sacsin* em N/TERT-1, HEK e HDFn foram utilizados dois anticorpos, um com reatividade para o N-terminal e outro para o C-terminal. Ambos os anticorpos

marcaram uma banda de alto peso molecular (520kDa) que muito provavelmente corresponde à forma nativa e funcional de *sacsin*. Uma proporção mais elevada da banda 520kDa em relação à proteína total foi observada nas células C6, seguida por HDFn, HEK e depois N/TERT-1 com o valor mais baixo. Bandas com peso molecular mais baixo foram observadas para todas as células e podem corresponder a formas truncadas da proteína *sacsin* ou deteções não específicas. No futuro, pode ser necessário caracterizar a função e atividade destas possíveis formas truncadas de *sacsin*, o que poderá fornecer mais informações sobre a função desta proteína na pele.

Em conclusão, devido ao facto dos queratinócitos N/TERT-1 expressarem a forma de maior peso molecular de *sacsin*, e conseguirem mimetizar a morfologia e as propriedades de epiderme nativa em cultura 3D, faz com que sejam o modelo celular ideal em trabalhos futuros para a criação de um modelo de pele *in vitro* da doença de ARSACS.

Palavras-chave: HaCaT, N/TERT-1, Modelo de epiderme *in vitro*, ARSACS, Sacsin

Table of Contents

Index of Figures

Index of Tables

List of Abbreviations

ALI	Air-liquid interface
ARSACS	Autosomal Recessive Spastic Ataxia of Charlevoix-Saguenay
BCC	Basal cell carcinomas
DAG	Diacylglycerol
EBS	Epidermis bullosa simplex
EGF	Epidermal growth factor
GAPDH	Glyceraldehyde 3-phosphate dehydrogenase
GFP	Green fluorescent protein
H&E	Hematoxylin and eosin
HDF	Human dermal fibroblasts
HEK	Human epidermal keratinocytes
HRP	Horseradish peroxidase
hTERT	Telomerase reverse transcriptase (human)
IFs	Intermediate filaments
IP3	Inositol 1,4,5-trisphosphate
K1	Keratin 1
K10	Keratin 10
K14	Keratin 14
K15	Keratin 15
KGF	Keratinocyte Growth Factor
KO	Knockout
MW	Molecular weight
NF	Neurofilaments
PBS	Phosphate-buffered saline
pI	Isoelectric point
PI3K	Phosphatidylinositol-4,5-bisphosphate 3-kinase
PIP2	Phosphatidylinositol 4,5-bisphosphate
PIP5K1	Phosphatidylinositol phosphate kinase
PKC	Protein kinase C
RhoA	Ras homolog family member A
SDS-PAGE	Sodium dodecyl sulphate–polyacrylamide gel electrophoresis
shRNA	Short-hairpin RNA
UV	Ultra-violet

1 Introduction

1.1. The skin is a three-dimensional dynamic structure

The skin is the largest organ of the human body and constitutes a barrier that protects the body from a range of external stressors and maintains homeostasis. It is composed of two main compartments, the dermis and the epidermis, both linked tightly by the dermo-epidermal junction (Fig. 1.1).

The epidermis is the outermost layer of the skin and the main responsible for the barrier function. It is a keratinized stratified squamous epithelium, predominantly composed of keratinocytes, but also melanocytes and Langerhans cells. Due to its direct exposure to environmental factors, epidermal cells are more susceptible to harmful effects, so keratinocytes are constantly dying and being replaced. Keratinocytes proliferate in the bottom layer of the epidermis *(stratum basale*) and move upwardly through several *strata* while they differentiate until they reach the *stratum corneum* (this process takes 2-4 weeks). The *stratum basale* is the epidermal layer closer to the dermis, characterized by a single layer of basal cells, precursors to the keratinocytes, which have a cuboidal shape and undergo constant proliferation. It is also at the *stratum basale* where melanocytes are present, producing the pigment melanin, essential to protect the cells from UV radiation. Above the *stratum basale* is the *stratum spinosum,* composed of 8-10 layers of cells and characterized by the presence of desmosomes, which give a spiny appearance to these cells. The desmosomes provide a tight connection between the cells, ensuring structural support [1].

The next layer is the *stratum granulosum* (3-5 layers of cells), where the keratinocytes produce large quantities of keratin, an intermediate filament that is the basic component protein of the skin. Keratinocytes also produce keratohyalin granules, which contain profillagrin, a precursor of filaggrin, the main histidine-rich protein that interacts with keratin to form fibrils that are responsible for the epidermis integrity[2,3]. Lamellar bodies containing a mixture of glycosphingolipids, phospholipids and ceramides are also very abundant and characteristic of this layer. As they move to the surface, keratinocytes start to lose nuclei and cytoplasmic organelles, becoming flatter. In areas with thick skin (palms, soles, and digits), there is an additional layer named *stratum lucidum.* It is a thin layer composed of flattened, dead cells, rich in a clear protein associated with lipids, known as eleidin[4].

The most superficial layer is the *stratum corneum*, composed of 18-20 layers of dead cells, preventing the entry of pathogens, the loss of water, and the mechanical wear of subjacent layers. The flattened scales that make up the *stratum corneum*, called corneocytes after losing their nuclei and organelles, are rich in keratin and are embedded in a lipidic layer released by the lamellar bodies[5–7]. Profilaggrin and loricrin, previously packed in the keratohyalin granules, are key proteins that allow the formation of the cornified envelope, which is a highly insoluble structure that replaces the plasma membrane of these terminally differentiated cells[8]. Terminal differentiation of keratinocytes is dependent on calcium concentration, playing a role in the secretion of lamellar bodies and in the apoptotic process that converts keratinocytes into corneocytes[9]. There is a calcium gradient through the epidermal layers, with lower calcium concentration in the bottom layers and higher in the upper layers. The calcium-sensing receptor (CaR) is a crucial player in this process, interacting with RhoA and Src family kinases, which in turn will form a stable E-cadherin–catenin complex in the membrane. Then, PI3Kand PIP5K1 are recruited to the complex and activate the Phospholipase-C (PLC-γ1)/PIP2 signaling cascade, which culminates with the production of second messengers IP3 and DAG. They induce the release of calcium from intracellular stores, activating PKC and turning on the transcription of the genes required for keratinocyte differentiation, such as Keratin 1 and 10, involucrin, transglutaminase-I, loricrin, and filaggrin[10–12].

The dermo-epidermal layer is a dynamic interface between the two different cellular compartments, providing not only adhesion and mechanical stability, but also influencing cell polarity, proliferation, migration, and differentiation of keratinocytes[13,14]. It provides anchorage of the epithelial cells to the dermal matrix with hemidesmosomes, expressing laminin 5 and collagen IV. Contrary to the epidermis, nerves, blood, and lymph vessels run through the dermis, besides other structures, such as hair follicles and sweat glands (Fig. 1.1). The primary cell constituent of the dermis is the fibroblast, which secretes collagen and elastin, among other proteins, the former being the main component of the dermal matrix. The dermis is divided into an upper papillary layer, containing loosely arranged collagen fibers and fibroblasts over a thick reticular layer with dense parallelly arranged collagen fibers and fewer fibroblasts. Directly beneath the dermis is the hypodermis, or subcutaneous layer, the tissue connecting the skin to the underlying fibrous tissue of bones and muscles. Fibroblasts and adipocytes are the main cell types in this layer[1,15].

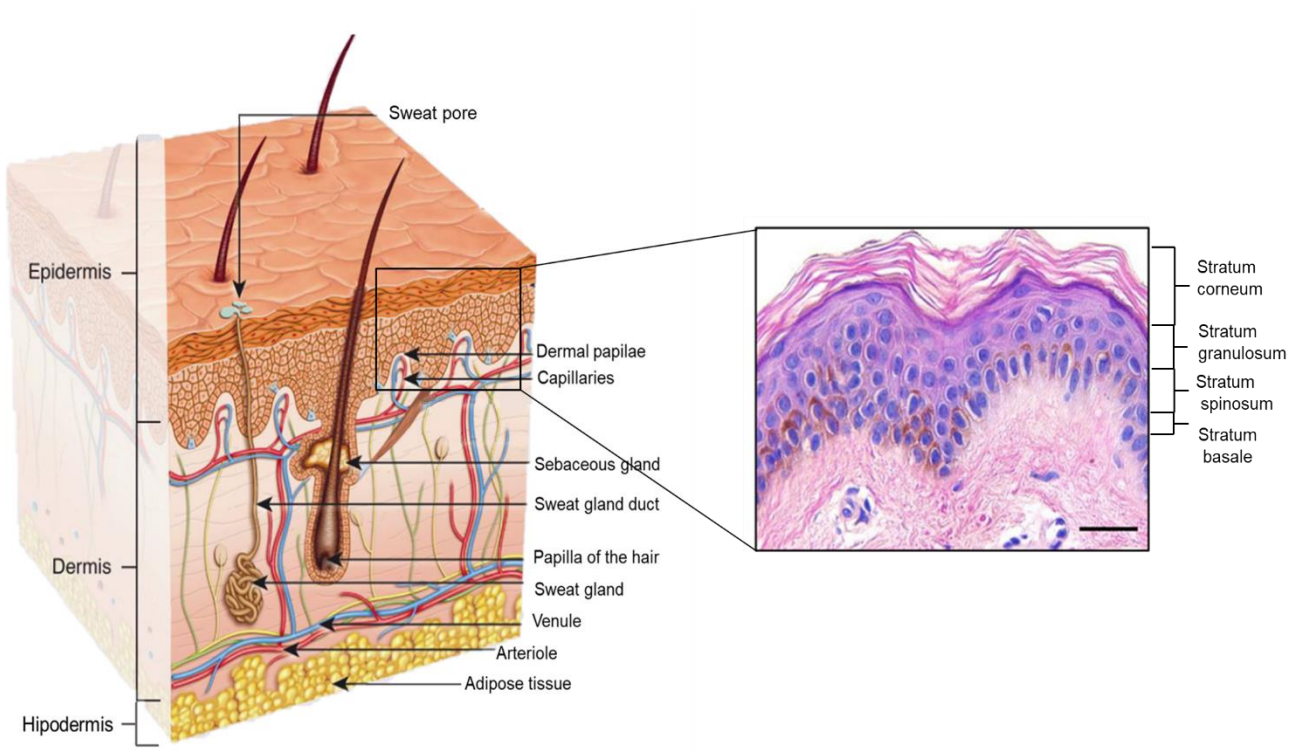

Figure 1.1 Morphological representation of human skin. On the left, there is a schematic representation of human skin, where the main structures of the dermis and epidermis are present, including sweat and sebaceous glands. On the right, there is a histological section of human skin (H&E staining) showing the four main layers in the epidermis: *stratum basale*, *stratum spinosum*, *stratum granulosum*, and *stratum corneum*. Adapted from Mathes, S.H. *et al*, 2014 and Roger, M. *et al*, 2019 [6,16].

1.1.1 Intermediate filaments are an integrative part of the epidermis

Intermediate filaments (IFs) are one of the main components of the cytoskeleton of mammalian cells, along with the microtubules and the actin microfilaments. IFs were first described in muscle cells and named according to their intermediate size between thin (actin) and thick (myosin) filaments, their diameter being approximately 10 nm[17]. In contrast to actin filaments and microtubules, IF proteins are a very heterogeneous family that are encoded by 70 conserved human genes [18]. According to their amino acid and DNA sequence homology, IFs can be divided into six subtypes, named from I to VI. Regardless of their subtype, all IF proteins show a conserved structure, divided into three segments: two nonhelical domains at the N-terminal and C-terminal, called head and tail domains respectively, and an alpha-helix central rod domain. The head and tail domains are mainly responsible for the interaction with IF-

associated proteins, while the rod domain is crucial in the first step of the IF assembly process[19]. This domain (300-330 aminoacids) contains 4 subdomains (1A, 1B, 2A, 2B), each one composed of sequential repeating units of seven aminoacids (heptads) where the 1st and 4th position are occupied by hydrophobic residues. This creates a hydrophobic region in each alpha-helix monomer, which determines dimerization[18].

Types I and II of the IFs are composed of keratins, consisting of 54 out of the total 70 human genes and representing the most abundant type of IF in all epithelia. Type I and type II keratins differ on sequence homology of the central rod domain, molecular weight (40-60 kDa for type I keratins and 50-70 kDa for type II keratins), and electrochemical properties (type I keratins are acidic, pI 4,5-6, while type II keratins are neutral or basic, pI 6,5-8,5)[20,21]. Keratins are expressed in a tissue-specific manner, hence their importance as biomarkers. For instance, throughout the epidermal differentiation process, different *strata* can be characterized by the keratins they express. The *stratum basale* is characterized by the expression of keratins 5 and 14, but their expression levels decrease towards the upper layers, accompanied by an increased expression of keratins 1 and 10[22,23].

In order to form the 10nm filaments, the first step is the formation of dimers with a coiled-coil structure through the interaction of the central rod domain. In the case of keratins, dimer formation occurs between the interaction of a monomer of a keratin type I and a monomer of a keratin type II in parallel orientation[24,25] (Fig. 1.2A). Then, dimers associate in an antiparallel fashion to form tetramers, which are the IFs building blocks[19,26]. Finally, tetramers associate laterally giving origin to unit length filaments (ULFs), whose successive longitudinal addition leads to the formation of IFs [19]. While actin filaments and microtubules grow by adding new monomers to the apical end, IFs are not polarized and can grow in both directions (i.e. they are apolar).

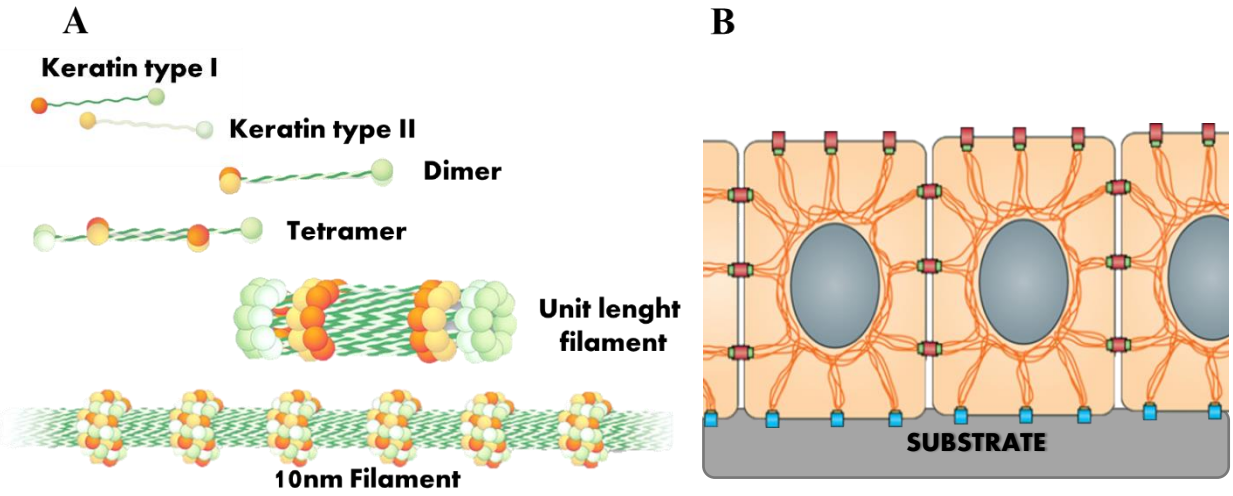

Figure 1.2 (A, B) Intermediate filaments formation and their role in maintaining epidermal structure. (A) Keratin dimers are formed by parallel association of two monomers (please note that the orange and green terminals are a schematic representation of the N- and C-terminal, respectively), one from a type I and the other from a type II keratin. Dimers form tetramers by an antiparallel arrangement, which then associate laterally to form unit-length filaments (ULFs). ULFs are longitudinally added to form the 10 nm intermediate filaments. Adapted from Yoon, S. and Leube, R., 2019[27]. (B) Keratin filaments are arranged in bundles in the cytoplasm, connecting neighboring cells through desmoplakin (green) in the desmosomes (red). Adherence to the underlying substrate is done via plectin (yellow) interaction, through hemidesmosomes (blue). Adapted from Haines, L. and Lane, E., 2012[23].

IFs have high stability and flexibility, being key players in structural support and tissue integrity. In stratified epithelia like the epidermis, keratin IFs form bundles in the cytoplasm that establish cell-to-cell connections through desmoplakin in desmossomes[28] and connect cells to their underlying substrate through hemidesmosomes by plectin interaction[29,30] (Fig. 1.2 B). This provides the formation of an extensive network fundamental for mechanical stress resistance of tissues and organs. Not only

are keratins fundamental in maintaining cell stiffness[31], but their impaired function impairs epidermis structure, as seen in some diseases. One example is epidermolysis bullosa simplex (EBS), a rare autosomal dominant condition caused by missense mutations in keratin 14 (type I) or keratin 5 (type II)[32,33], which are the most abundant pair of keratins expressed in the *stratum basale* of the epidermis. This disease is characterized by skin blistering due to mechanical trauma that causes the rupture of keratinocytes near the dermal-epidermal junction[32]. This fragility arises from keratins' defective mechanical properties and some mutations have also been linked to a reduction in the expression of components of the desmosome, resulting in decreasing tissue stability[34,35].

1.1.2 Reconstructed skin models: Important tools for research and development

In recent years, there has been growing ethical and legal pressure on the use of animals for research, clinical, and industrial purposes, including the prohibition in the European Union of animal testing of cosmetical products and active ingredients for cosmetical usage (Cosmetics Regulation EC No 1223/2009). Apart from this, frequently used animal models, such as rodents, have different skin characteristics, often producing results that cannot be translated to humans, thus leading to increasing demand for *in vitro* skin models. When compared to two-dimensional (2D) cell cultures, three-dimensional (3D) models are able to better recapitulate *in vivo* physiology, allowing cell-to-cell and extracellular matrix interactions[36–38]. Depending on the desired application and on the degree of complexity needed, there are two main categories of three-dimensional skin equivalent models: reconstructed human epidermal models, or full-thickness skin models. Both epidermal models and full-thickness skin models are usually generated using scaffolds that provide support, which have structural, mechanical, and functional properties similar to the biological tissue.

Reconstructed human epidermal models are normally generated by seeding keratinocytes on a scaffold and providing the conditions necessary to obtain a stratified epidermis. To promote differentiation, the epidermal model is most frequently exposed to an air-liquid interface, essential to achieve normal epidermal morphology and barrier function[39,40]. Growth factors and other signaling molecules involved in epidermal differentiation, such as calcium, are also used. A molecule with particular relevance is L-ascorbic-acid, or vitamin C, inducing keratinocyte differentiation by a mechanism similar to calcium-induced differentiation. Moreover, L-Ascorbic acid also increased intracellular glutathione levels, helping cells to maintain homeostasis and antioxidant levels[41].

The dermo-epidermal layer is a complex mixture of proteins secreted due to the interaction of keratinocytes and fibroblasts[13]. As such, the scaffold used to seed the keratinocytes must have similar mechanical and biological properties to this layer. The most common scaffolds used are synthetic polymers, such as polycarbonate and polystyrene, which allow the tailoring of their physical properties, such as porosity and elasticity, to meet specific applications. Nonetheless, the absence of interaction with fibroblasts can be one of the drawbacks of reconstructed epidermal models, which can sometimes be overcome by the use of an exogenous coating, usually collagen, in order to enable the adherence of keratinocytes to the scaffold[39,42]. Using a dermal component can also be a solution, having the advantage of mimicking the human skin more closely.

The first full-thickness skin models involved the seeding of keratinocytes into decellularized skin, namely pig skin or human skin[39,43]. In recent times, hydrogels have become a popular technique for developing skin models. These are normally collagen I scaffolds into which fibroblasts are cultured[44,45]. In addition to collagen, other proteins present in the extracellular matrix can be used, such as fibrin[46]. Although the usage of natural polymers to generate hydrogels resembles *in vivo* architecture, these generally do not have the ideal mechanical properties for long-term cell cultures, sometimes exhibiting physical contraction, distortion, and enzymatic degradation[44,47]. Additionally, the use of animal-produced collagen can decrease reproducibility.

Alternatively, an option is to generate artificial scaffolds that allow the growth and proliferation of fibroblasts, thus allowing them to produce their own extracellular matrix. Polystyrene scaffolds have been developed for this application, showing promising results[48]. Additionally, these types of scaffolds also have the advantage of allowing the construction of a fully humanized skin model, without the need for animal byproducts, therefore making a valuable tool for researching, testing, and evaluating new therapies and drugs.

Another important factor to take into consideration is the type of cells used in skin models. Primary human skin cells, isolated from standard surgical procedures, are the most common type of cells used to generate full-thickness skin or epidermal models. Primary cells were shown to produce skin models that successfully mimic human skin, creating a functional dermal compartment and a stratified epidermis[16,49,50]. However, primary cells present a few disadvantages, not only because of donor variation and unpredictability but also due to the restricted proliferation capacity and senescence onset.

Immortalized cell lines could overcome these issues. The HaCaT cell line is a spontaneously immortalized keratinocyte cell line widely used in research. It was first created in 1988, derived from a region surrounding a melanoma from a 62-year-old patient[51]. This cell line is aneuploid, but non-tumorigenic, despite showing a transformed phenotype *in vitro*. Although it maintains some differentiation capacity, some attempts to use it to form epidermis have resulted in disorganized morphology[52–55]. A study that used mechanical stress to induce differentiation of HaCaT was able to reconstruct the epidermal morphology, with *stratum corneum* formation[56]. Another option is to use hTERT-immortalized keratinocytes. In theory, immortalization with hTERT cDNA, which encodes for the catalytic subunit of human telomerase, prevents telomere shortening (this is progressive after each cell cycle), increasing the life span of primary cells[57]. Skin models using hTERT-immortalized keratinocytes have been successfully generated[58,59].

There are commercially available epidermal models, such as EpiDerm™ (MatTek, Ashland, MA, USA) and Episkin (L´Oreal; SkinEthic, Nice, France), and full-thickness skin models, such as Labskin (Innovenn, Dublin, Ireland) and Phenion® Full-Thickness Skin Model (Henkel AG & Co. KGaA, Düsseldorf, Germany). However, these can be costly and do not allow tailoring to meet specific research needs [6,60]. Bearing this in mind, the development of skin models that can be generated using reproducible protocols and modified to meet specific needs is important to expand the range of applications and spread their use. Some important applications of skin models are the recapitulation *in vitro* of a specific disease phenotype, to allow further insight into the pathophysiology mechanisms and the development of new therapies.

1.2. Autosomal recessive spastic ataxia of Charlevoix-Saguenay (ARSACS)

Autosomal recessive cerebellar ataxias are a group of heterogeneous and rare diseases whose symptoms have mostly an early onset, ranging from the first years of age to early adulthood [61,62]. Clinical manifestations vary from cerebellar syndromes to sensorimotor neuropathy, ophthalmological disturbances, involuntary movements, seizures, cognitive dysfunction, skeletal anomalies, and cutaneous disorders [63]. Among these diseases, the autosomal recessive spastic ataxia of Charlevoix-Saguenay (ARSACS) (OMIM:270550) is considered to be among the three most frequent types of autosomal-recessive ataxias worldwide, after Friedreich ataxia (FRDA) and Ataxia Telangiectasia [63,64]. FRDA has an incidence frequency ranging from 1 in 30,000 to 1 in 50,000 in most populations, while Ataxia Telangiectasia affects 1 in 40,000 in the United States of America [63,65,66]. Worldwide prevalence of ARSACS is unknown, but in Quebec (Canada), the incidence at birth is 1:1,932[67].

ARSACS was first described in the Charlevoix-Saguenay region of Quebec (Canada) in the 70s of the previous century [68]. It is estimated to have a carrier frequency of 1/22 in this region and an estimated prevalence of 1/484, but about 200 cases have been reported worldwide, more specifically in Europe, Asia, Africa, and North and South America [66,69]. As the name suggests, ARSACS patients present signs of spasticity in the lower body at an early age, generally between the age of 12 and 24 months, progressing through the patients' life [63,64,68]. Patients also suffer from a lack of voluntary coordination of muscle movements, known clinically as ataxia, which can manifest through gait abnormality, speech changes, and abnormalities in eye movements. In early adulthood, motor axonal-demyelinating polyneuropathy signs become more evident, such as an increase in the muscle tone in the lower extremities and hyperreflexia, causing weakness, numbness, and pain [64,66]. Intellectual deficit and retinal damage, such as retinal ganglion cell and nerve fiber hyperplasia, have also been reported in some patients[64,70]. These symptoms are common among Quebec patients, but the disease phenotype can be milder in patients outside this region, with only some of the symptoms present[71]. Patients usually become dependent of the wheelchair around 41 years of age (age ranges from 17-57), with death occurring at the average age of 51[64].

ARSACS results from the degeneration of Purkinje neurons in the cerebellum, the part of the brain whose functions include motor coordination and balance [72]. Magnetic Resonance Imaging (MRI) shows atrophy of the superior cerebellar vermis from a young age (Fig. 1.3 A), but the cortex can also be affected, showing bilateral parietal cerebral atrophy [64,71]. Post-mortem examinations have also shown swollen thalamic and cerebellar cortical neurons, accompanied by the presence in most cells of lysosomes with lipofuscin-like granules[73]. Interestingly, lipofuscin granules have also been seen in skin biopsies of ARSACS patients[74] (Fig. 1.3 B). Lipofuscin is non-degradable cellular debris that accumulates with increasing age in postmitotic cells, which has also been seen in early degenerating neurons in protein misfolding disorders, such as Alzheimer's disease[75].

There is no known treatment for ARSACS, and the clinical approach focuses on palliative care, mainly through the use of physiotherapy and pharmacotherapy to control some of the symptoms, particularly spasticity.

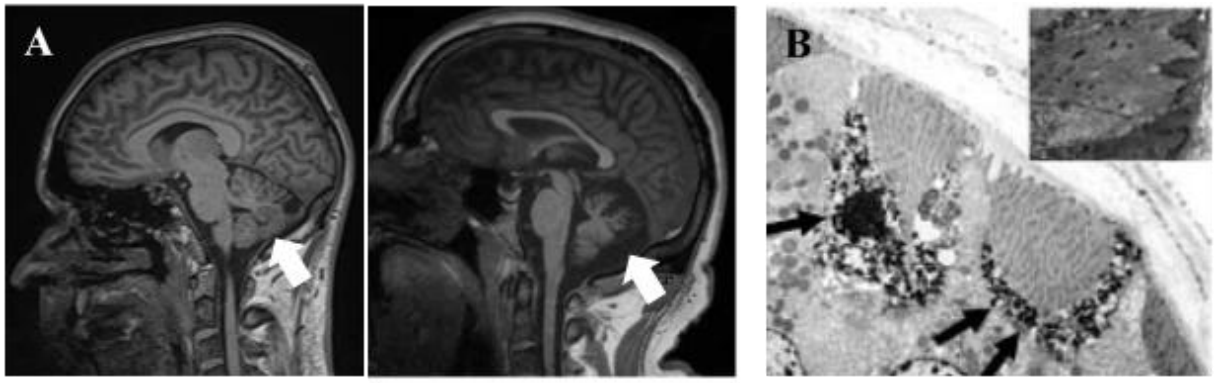

Figure 1.3 (A, B) Cerebellar atrophy and skin lipofuscin granules are symptoms of ARSACS. (A) Saggital MRI images from a 35-year-old man without any structural abnormalities (left) and from a 37-year-old male ARSACS patient showing marked atrophy in the superior cerebellar vermis (right). In both images, the cerebellum is marked with an arrow. Images were retrieved from Dimitrov, I. et al, 2018[76] and Stevens, J. at al, 2013[74]. (B) Ultrastructural images show lipofuscin deposits in basal epidermal cells of a skin biopsy from a 37-year-old male ARSACS patient (arrows). A control image is shown (age-matched control) above where no lipofuscin is detected. Images were retrieved from Stevens, J. et al, 2013[74].

1.2.1. Mutations in the *SACS* gene cause ARSACS phenotype

The *SACS* gene is located in chromosome 13 (13q12.12) [77–79]. The gene contains a giant exon spanning more than 12.8 kb, originally thought to be the only exon in the gene [80]. Eight additional smaller exons were discovered in the region upstream of the giant exon, expanding the exon count to 9 and the total

size of the gene to 13.7 kb[81–83,18]. However, the number of exons can be higher according to bioinformatical analysis, predicting a total number of exons of 13(GenBank gene ID: 26278). ARSACS is caused by mutations of both alleles in the *SACS* gene. Originally, only two mutations were found in the affected population of Charlevoix-Saguenay (explaining 92.6% and 3.7% of carrier chromosomes), suggesting a founder effect [79,80]. From these two mutations, the most frequent is a single-base deletion at position 6,594 (g.6594delT), resulting in a frameshift alteration and the introduction of a premature stop codon. The other mutation, which is present in minor abundance and usually in heterozygosity with the major mutation, is a nonsense mutation (g.5254C→T) resulting in the substitution of an arginine by a premature stop codon. However, more than 200 mutations have been identified around the globe [64,69,84], including 5 additional recurrent mutations in Quebec [85]. Predictably, most mutations are located in the giant exon, due to its larger size[83]. The high degree of mutation heterogenicity has been linked to different phenotypes and disease severity[69,71]. Sacsin knockout mice reproduce many ARSACS features, such as an early onset syndrome with motor, cerebellar and peripheral nerve dysfunctions, indicating that ARSACS is caused by sacsin loss-of-function. However, the function of sacsin remains unclear.

1.2.2. Sacsin has a putative chaperone-like function

The *SACS* gene encodes a 4,579 aminoacids protein[81], sacsin (Uniprot ac. number: Q9NZJ4), which has a molecular mass of 521 kDa and is composed of multiple domains (Fig. 1.4). Near the N-terminus, there is a ubiquitin-like (UbL) domain that interacts with the 19S cap of the 26S proteasome subunit [81]. Three repeated regions have been identified (SIRPT1, SIRPT2, and SIRPT3) that cover approximately 84% of the protein sequence[86]. Each of these repeated regions contains three subrepeats, sr1, sr2, and sr3, with SIRPT1 and SIRPT3 containing an additional region, srX. It was previously described the presence of a supra-domain in triplicate near the N-terminus of sacsin, termed "sacsin repeating region" or SRR[87], that is now known to include sr1 and sr2 subrepeats. Each sr1 contains a HATPase_c (Histidine kinase-like ATPases) domain, which is homologous to the ATP binding domain of an Hsp90-like co-chaperone. This architecture suggests that sacsin could work as a co-chaperone[86,87]. The sr3 and srX regions do not present any similarity with known domains, thus having an unknown role. However, a purified region of sacsin corresponding to SIRPT1 exhibits chaperone-like activity by enhancing luciferase refolding efficiency *in vitro*[88], which may indicate that sr3 and srX may be involved in the chaperone function. The possible function of sacsin as a chaperone is further supported by the presence of 3 additional domains usually associated with protein quality control near the C-terminus (XPCB, DnaJ and HEPN). The XPCB (Xeroderma Pigmentosum Complementation group C Binding) domain interacts with the Ube3A ubiquitin-protein ligase[89], which is associated with protein ubiquitination and degradation by the proteasome. The DnaJ domain interacts with members of the Hsp70 chaperone family[81,88], known to be involved in the cellular response to protein aggregation in neurodegeneration. And, finally, the HEPN (Higher Eukaryotes and Prokaryotes Nucleotide-binding) domain can bind nucleotides and mediate sacsin dimerization[90,91].

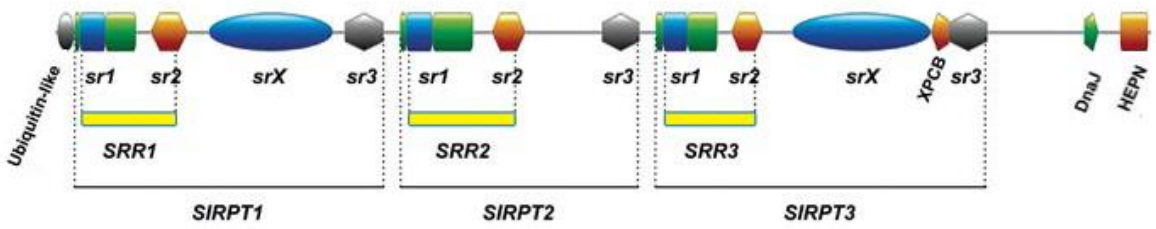

Figure 1.4 Domains and subrepeats present in the protein sacsin. From N-terminus to C-terminus (left to right): Ubiquitin-like (UbL) domain; three major repeated regions SIRPT1, SIRPT2, and SIRPT3; XPCB domain; DnaJ domain; HEPN domain. Each SIRTPT contains three subrepeats, sr1, sr2, and sr3, with SIRPT1 and SIRPT3 containing an additional region, srX. Adapted from Romano et al. 2013 and Li et al. 2015[86,92].

Due to sacsin´s extremely large size, no structures of the entire protein have been resolved. However, the structures of four isolated domains have been determined: the HEPN domain[91], the DnaJ domain[81], the sr1 domain of SIRPT1[93] and the Ubl domain[93]. These structures did not only support the data resulting from the sequence analysis mentioned above but also provided new insights into the effect on the protein structure of some of the mutations that occur in ARSACS patients. The architecture of the sr1 domain revealed that some missense mutations occurring in this region (R272H, R272C, and T201K) disrupt protein folding[93]. The N4549D mutation, which is localized in the HEPN domain also interferes with protein folding and dimerization, eliminating its nucleotide-binding activity [91]. However, not all mutations studied were shown to interfere with the protein structure[81,93].

1.2.3. Sacsin plays a role in mitochondrial function and intermediate filament organization

Apart from its putative chaperone-like role, sacsin cellular function remains unclear. Sacsin presents the highest expression in the central nervous system, but it has also been seen to be expressed in most tissues, including organs of the reproductive system and the skin[81,94,95]. On a cellular level, sacsin was shown to be predominantly cytoplasmic, with a proportion localizing to the outer membrane of the mitochondria [81,96]. Sacsin is also implicated in mitochondrial dynamics and morphology. ARSACS patients' fibroblasts (non-detectable sacsin expression) and sacsin knockout cell lines show an excessively interconnected mitochondrial network and mitochondria with a "balloon-like" morphology, due to decreased mitochondrial fission. Moreover, the loss of sacsin in neurons leads to mitochondria accumulation in the soma and proximal dendrites, leading to an abnormal dendritic morphology that precedes Purkinje cell death [96]. Dysfunction in mitochondrial bioenergetics has also been observed in ARSACS patients, as a result of reduced respiratory chain activities and mitochondrial ATP synthesis, accompanied by an increase in reactive oxygen species (ROS) and oxidative damage[97]. Mitochondrial fission is essential for the turnover of damaged parts in the mitochondrial network, preceding selective degradation by mitophagy[98]. Loss of sacsin decreases the number of dynamin-related protein 1 (Drp1) foci present in mitochondria, which is a protein recruited to division sites and a fission mediator[99,100]. In addition to this, sacsin is likely to be involved in the fusion of the autophagosome with the lysosome, necessary to create the autolysosome and to promote cargo degradation by lysosomal hydrolases[101].

Studies in sacsin knockout mice revealed anomalous accumulations of neurofilament (NF) bundles in the somatodendritic regions of some neuronal populations, similarly to what was also observed in ARSACS patients[102,103]. Sacsin can also affect the organization of intermediate filaments (IFs) other than NFs, such as vimentin. Vimentin aggregation had a cage-like appearance in cells where sacsin expression was diminished and in ARSACS patients fibroblasts[104]. Furthermore, cellular organelles, including mitochondria, were displaced to the periphery of vimentin accumulations, and there was also evidence for alterations in the autophagic activity. The IF architecture could be restored via the expression of full-length sacsin or the SIRPT1 and DnaJ domains[103]. In conclusion, sacsin ablation disrupts normal IF architecture, and this effect may be connected to the mitochondrial dysfunction observed in ARSACS.

2 Objectives of this work

Despite the existing knowledge about sacsin structure and function, a lot is still unknown about this protein and how it causes the symptoms underlying ARSACS disease. Advances in this topic might contribute to the development of therapies that could cure or tackle some of the symptoms to ensure a better quality of life for the patients. Considering that alterations in the skin of ARSACS patients have been previously reported[74], generating a skin model that recapitulates ARSACS features could be an important tool in this field of study. By taking advantage of 3D tissue culture technology, the first aim of this project is to develop and characterize novel 3D epidermal models using keratinocyte immortalized cell lines. Secondly, we aim to explore the role of sacsin in human skin cells in order to determine if it is possible to develop a skin model with an ARSACS phenotype.

3 Materials and methods

3.1 Reagents

Dulbecco's Modified Eagle Medium (DMEM), fetal bovine serum (FBS), Epilife medium, Human Keratinocyte Growth Supplement (HKGS), penicillin-streptomycin (10,000 U/mL) (Pen/Strep), bovine pituitary extract (BPE), Keratinocyte- Serum-Free Medium (K-SFM), phosphate-buffered saline (PBS), keratinocyte growth factor (KGF) and 0,05% trypsin/EDTA were purchased from Gibco® (Waltham, MA USA). Trypan blue solution 0,4%, 10 % neutral buffered formalin solution, HistoChoice® clearing agent, Proteinase K, L-ascorbic Acid and BSA (bovine serum albumin, ref.112018) were acquired from Sigma-Aldrich (St. Louis, Missouri, USA). Sacsin shRNA (h) Lentiviral Particles (cat. no. sc-61489-V), Control shRNA Lentiviral Particles (cat. no. sc-108080), Polybrene (cat. no. sc-134220), and sacsin CRISPR/Cas9 KO plasmid (cat. no. sc-404592) were obtained from Santa Cruz Biotechnology (Dallas, Texas, USA). ProLong™ Gold Antifade Mountant with DAPI, ECL Western Blotting Substrate, and horseradish peroxidase-conjugated goat anti-rabbit IgG (H+L) (cat. no. A16096) were purchased from Thermo Fisher Scientific (Waltham, MA, USA). The mouse monoclonal IgG1 anti-keratin Keratin 10 (cat. no. 11414) was acquired from Progen Biotechnik (Heidelberg, Germany). The mouse monoclonal IgG3 anti-Cytokeratin 14 (cat. no. ab7800) was acquired from Abcam (Cambridge, UK). The following antibodies were purchased from Santa Cruz Biotechnology (Dallas, Texas, USA): mouse monoclonal anti-sacsin IgG2B (cat. no. sc-515118), and mouse monoclonal anti-GAPDH (cat. no. sc-47724). Rabbit polyclonal IgG anti-keratin 15 (cat. no. SAB4501658), mouse monoclonal IgG1 anti-involucrin (ref. SAB4200794), Goat polyclonal FITC-labeled anti-mouse IgG (cat. no. F0257), and rabbit polyclonal anti-sacsin IgG (cat. no. ABN1019) were purchased from Sigma-Aldrich (St. Louis, Missouri, USA).

3.2 Cell culture

The HaCaT cell line was originally obtained from DKFZ, Heidelberg/Germany[51]. The N/TERT-1 cell line, previously established by Dickson et al.[105], was kindly provided by Dr. van den Bogaard (Radboud University, Nijmegen, the Netherlands). Human dermal fibroblasts (neonatal) (P10857, Innoprot, Bizkaia, Spain) were maintained in DMEM medium supplemented with 10% FBS and 1% Pen/Strep. Human epidermal keratinocytes (neonatal) (C0015C, Gibco ®, Waltham, MA USA) were cultured in Epilife medium, 1% Pen/Strep, 1% HKGS, containing 0.2% v/v BPE, 0.01 µg/mL recombinant human insulin-like growth factor-I, 0.18 µg/mL hydrocortisone, 5 µg/mL bovine transferrin, 0.2 ng/mL human epidermal growth factor (EGF), with 0,06mM $CaCl_2$. HaCaT cells were cultured in DMEM medium, supplemented with 10% FBS and 1% Pen/Strep, or Epilife medium, supplemented with 1% Pen/Strep, 1% HKGS, with 0,6mM or 0,03mM $CaCl_2$. The N/TERT-1 cell line was cultured in K-SFM medium, 1% Pen/Strep, supplemented with BPE (25 µg/ml), EGF (0.2 ng/ml) and 0,4 mM $CaCl_2$. All the procedures regarding cell culture and handling were done following procedures for aseptic technique and using a vertical laminar flow chamber of biosafety class II type A/B3 (Nuaire, Doncaster, England).

Cells were stored in liquid nitrogen (vapor phase) until usage. Cells were thawed by placing the cryopreservation tube in ice and then transferring to a water bath at 37 ºC until there were no visible ice crystals. Medium was added to dilute the freezing solution and after centrifugation (300g for 5 minutes at room temperature), cells were resuspended in the appropriate medium volume and transferred to a T-flask, kept at 37ºC, 5% CO_2. The medium was changed the day after, if needed. Cells were passaged

once or twice a week when they reached the desired confluency. Keratinocyte differentiation has been described in the literature to be mediated by cell-to-cell contact[106], so HaCaT cells and human primary keratinocytes were kept at a density lower than 70% confluence. N/TERT-1 keratinocytes were kept at confluency below 35%. To pass and expand the cell culture, T-flasks were first washed with PBS. After this, cells were detached by trypsin addition (0,05% Trypsin/EDTA) and incubated at 37ºC, 5% CO_2 for 5-10 minutes, and trypsin was neutralized by the addition of serum-containing culture media. After centrifugation (300g for 5 minutes at room temperature), cells were resuspended in the desired volume and the number of viable cells was counted. This was done by diluting an aliquot of the cell suspension in trypan blue 0,4% solution and counting the number of viable cells in four squares of a Neubauer Chamber. After calculating the cell concentration, the desired number of cells was transferred to one or more T-flasks (dilution range 1:2-1:5). To freeze cells, after centrifugation the pellet was resuspended in 1mL of freezing solution (FBS, 10% Dimethyl sulfoxide). The vials were stored at -80ºC for 24h in a controlled-rate (-1ºC/minute) freezing container before being stored in liquid nitrogen.

3.3 3D epidermal equivalents generation

To build a 3D epidermis, HaCaT and N/TERT-1 cell lines were used. For the HaCaT cell line, two different culture media (Epilife and DMEM) were tested in order to optimize the 3D epidermal equivalent model protocol. The desired number of cells (ranging from $1,5x10^5$ to $5x10^5$ cells) was seeded onto the inserts (Millicell® PIHP 012050, Merck Millipore, Darmstadt, Germany) in a volume of 500 µl in High Calcium Medium (Epilife with 1,5mM $CaCl_2$ or DMEM) (Fig 3.1). High Calcium Medium was also added to the well. After 24 hours, the inserts were raised to air-liquid interface, which consisted of the complete removal of the medium inside the insert (Fig. 3.1). The medium of the well was replaced by Air-Liquid Interface (ALI) medium, which consisted of Epilife Medium 1,5mM $CaCl_2$ or DMEM medium, supplemented with 1% HKGS, 1%PenStrep, 100ug/mL L-ascorbic Acid, 100ppm KGF. The medium was changed every 2-3 days.

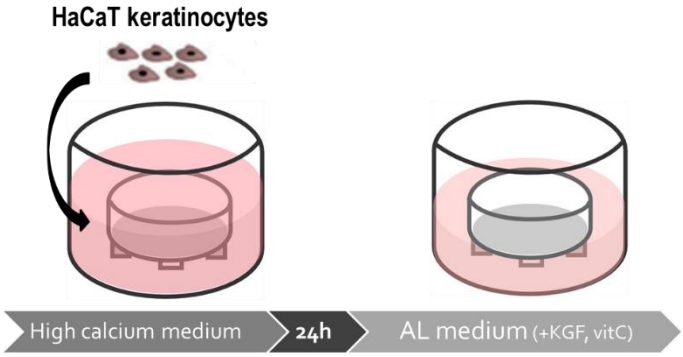

Figure 3.1 Schematic representation of 3D epidermis equivalent protocol for the HaCaT cell line. First, keratinocytes were cultured in the insert in high calcium medium. After being submerged for 24h, the medium was removed and the inserts were raised to air-liquid interface by removing the medium from the inside (leaving the inert polycarbonate membrane where the keratinocytes were seeded dry) and adding air-liquid interface medium to the outside of the insert. The medium was changed every 2-3 days.

The protocol used to produce a 3D epidermis with N/TERT-1 keratinocytes had a few modifications (Fig. 3.2). Previously to seeding the cells, the inserts (Millicell® PIHP 012050, Merck Millipore, Darmstadt, Germany) were coated with rat tail collagen type I (Corning®, Corning, New York, USA). Briefly, collagen type I was diluted in 70% ethanol (final concentration of 0,75mg/ml), and 100 µl were distributed onto the inserts, which were left to dry overnight in a cell culture hood. N/TERT-1 keratinocytes were seeded onto the insert in the same medium used for 2D cell culture (K-

SFM medium, supplemented with 25 µg/ml BPE, 0.2 ng/ml EGF, and 0,4 mM $CaCl_2$) and the same medium was added to the outside of the insert. After 48h, the medium inside and outside of the insert was replaced by high calcium medium (K-SFM medium supplemented with 25 µg/ml BPE, 0.2 ng/ml EGF, and 1,5 mM $CaCl_2$). The air-liquid interface was done after 24h by completely removing the medium inside the insert and adding ALI medium (K-SFM medium supplemented with 25 µg/ml BPE, 0.2 ng/ml EGF, 1,5 mM $CaCl_2$, 50µg/mL L-ascorbic Acid, 10ng/ml KGF). The medium was changed every 2-3 days.

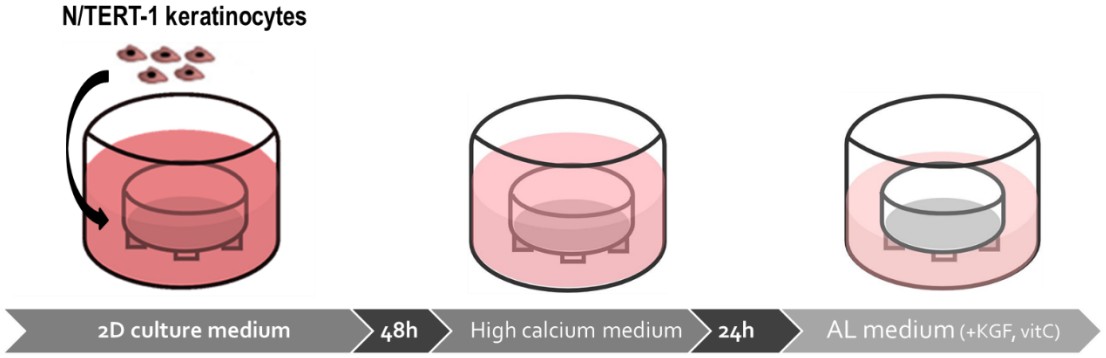

Figure 3.2 Schematic representation of 3D epidermis equivalent protocol for the N/TERT-1 cell line. Keratinocytes were cultured in the insert in the same medium used to establish the 2D cell culture. After 48h, the medium was replaced by medium with high calcium concentration. Inserts were raised to air-liquid interface 24h after by adding air-liquid interface medium to the outside of the insert and leaving the inert polycarbonate membrane, where the keratinocytes were seeded, exposed to the air. The medium was changed every 2-3 days.

3.4 Histology and immunohistochemical analysis

Inserts were fixed in 10 % neutral buffered formalin solution for 24 hours. The membranes used to grow the 3D epidermis or the 3D skin equivalents were then removed from the inserts using a scalpel and were placed in histological cassettes. Paraffin embedding, sectioning, hematoxylin and eosin (H&E), and Ki67 staining were done by the Histopathology Unit of Instituto Gulbenkian de Ciência (IGC). Briefly, the tissue was first dehydrated by passing it through increasingly higher concentrations of ethanol (from 0% to 100%). After this process was completed, the ethanol was replaced with xylene, followed by infiltration with paraffin wax, and embedded. The paraffin blocks were then sectioned (4 µm sections) using a microtome. Because most staining solutions are water-soluble, the sections were rehydrated by passing through ethanol and increasing concentrations of water (0% to 100%). For the H&E stain, the hematoxylin nuclear stain was applied first, then rinsed with water, and "blued", which was done by treatment with an alkaline solution that gives hematoxylin a dark blue color. Afterward, the section was stained with eosin, dehydrated again, and placed in xylene. For the Ki67 antibody staining, after heat antigen retrieval, sections were washed with PBS/0.1% Tween-20. After applying the blocking solution, sections were incubated overnight at 4ºC with the Ki67 antibody. On the day after, sections were washed again and incubated with the HRP-conjugated antibody. DAB (3,3'Diaminobenzidine) substrate was then added, and after the sections developed, they were counterstained with hematoxylin and dehydrated. Finally, sections were mounted in slides with mounting media and covered with a coverslip.

3.5 Immunofluorescence

The following antibodies were used to stain sections from paraffin blocks: mouse monoclonal IgG1 anti-keratin Keratin 10 (1:10); mouse monoclonal IgG3 anti-Cytokeratin 14 (1µg/ml); rabbit polyclonal IgG anti-keratin 15 (1:100); mouse monoclonal IgG1 anti-involucrin (1:200); Goat

polyclonal FITC-labeled anti-mouse IgG (1:500); Goat polyclonal Alexa Fluor 488-labeled anti-rabbit IgG (1:500).

To dewax paraffin sections (4 µm sections) and to prepare them for antibody probing, they were placed at 65ºC for 30 minutes and treated with HistoChoice® clearing agent for 10 minutes. The sections were then gradually hydrated with ethanol solutions with increasingly higher concentrations of water (100%, 96%, 70% ethanol) for 5 minutes each. This was followed by 4 cycles of heating for 2 minutes (microwave, 800W) and cooling at room temperature for 3 minutes in citrate buffer (pH 6). An additional step of incubation with Proteinase K (20µg/ml) for 15 minutes was done for the sections stained with anti-K10 and anti-K15 antibodies. The sections were washed for 10 minutes in PBS (3 cycles) and incubated with PBS/1% Triton X-100 for 15 minutes. This was followed by incubation with a blocking solution (PBS/1%BSA) for 15 minutes or 1h in the case of anti-K14 antibody. The primary antibodies were incubated overnight at 4ºC. A negative control (without primary antibody) was done for every section, by incubating overnight at 4ºC with blocking solution (PBS/1%BSA). The next day, 3 washes with PBS (10 minutes each) were carried out, followed by incubation with the secondary antibodies diluted in PBS/1%BSA for 2 hours at room temperature. The sections were washed again in PBS (3x10 minutes), mounted with ProLong™ Gold Antifade Mountant with DAPI, and covered with a coverslip. The slides were stored at 4ºC in the dark.

3.6 Immunoblotting

To extract total proteins, cells were washed with ice-cold PBS 1x and cold lysis buffer (50 mM Tris-HCl, 150mM NaCl, 1% (v/v) NP-40, pH 7,5) was added, containing cocktails of protease and phosphatase inhibitors (NZYTech, Lisbon, Portugal). Cells were harvested by scraping and incubated in ice for 10 minutes before sonication (amplitude 10%, 1 pulse of 5s) using a Branson 450 D Sonifier (Branson Ultrasonics Corporation, Danbury, Connecticut, USA). Then, cell lysates were centrifuged at 10000g for 10 minutes at 4ºC and the protein fraction (supernatant) was collected. Protein quantification was done by the Bradford method[107]. Briefly, protein extracts were incubated for 10 minutes with Bradford reagent (AppliChem Panreac, Milan, Italy) in the dark and the absorbance was measured at 595nm using a SpectraMAX 340 microplate reader (Molecular Devices Corporation, Sunnyvale, CA, USA). The amount of protein in each extract was calculated by generating a standard curve with known concentrations of bovine serum albumin (BSA) (Pierce™, Thermo Fisher Scientific, Waltham, MA, USA). C6 and C6 *SACS* -/- protein extracts were kindly provided by Fernanda Murtinheira from Dr. Federico Herrera's Laboratory.

Before separation by SDS-PAGE, the protein extracts were denatured by adding loading buffer [10% (v/v) 2- mercaptoethanol, 4% (v/v) sodium dodecyl sulfate (SDS), 0.004% (v/v), 20% (v/v) glycerol, 0.004% (v/v) bromophenol blue, 0.125 mM Tris-HCl] and incubating for 5 minutes at 95ºC, followed by 5 minutes in ice. Proteins were separated by 15%, 10%, or 6% SDS-PAGE, depending on the molecular weight of the protein of interest (e.g. Sacsin was separated by 6% SDS-PAGE, while 10-15 % was used to visualize intermediate filaments and GAPDH), and transferred to a nitrocellulose membrane (GE Healthcare, Chicago, IL, USA) at 100V for 1 hour. To visualize protein bands and confirm a correct transfer to the membrane, 0.1% (w/v) Ponceau S in acetic acid staining solution was used. After washing with Milli Q water, membranes were blocked with 5% (w/v) non-fat dry milk in TBS-T (50 mM Tris-HCl, 150 mM NaCl, pH 7.6, 0.1% Tween 20) for 1 hour at room temperature. Membranes were washed with TBS-T, and subsequentially incubated overnight at 4ºC with the following primary antibodies, diluted in 3% (w/v) BSA, 0.05% (v/v) sodium azide, in TBS-T: mouse monoclonal anti-sacsin IgG_{2B} (1:500), rabbit polyclonal anti-sacsin IgG (1:500), mouse monoclonal anti-GAPDH (1:1000); mouse monoclonal IgG1 anti-keratin Keratin 10 (1:500). Membranes were rinsed again with TBS-T (3x 10min) and further incubated with horseradish peroxidase-conjugated goat

anti-mouse IgG (H+L) (1:10000) or horseradish peroxidase-conjugated goat anti-rabbit IgG (H+L) in 5% (w/v) non-fat dry milk in TBS-T, for 1 hour at room temperature. Membranes were visualized with ECL Western Blotting Substrate and images were obtained in a ChemiDoc XRS+ system (Bio-Rad, Hercules, CA, USA).

3.7 Lentiviral transduction

To knockdown sacsin expression in HaCaT cells, sacsin shRNA (h) Lentiviral Particles and Control shRNA Lentiviral Particles were used according to the manufacturer's instructions. Briefly, HaCaT cells were cultured in complete DMEM medium (10%FBS, 1%Pen/Strep), and transduction with the lentiviral particles was done at 80% confluency. For the lentiviral transduction experiment, only DMEM medium was used, as it is suitable for 2D HaCaT culture. A mixture of 5µg/mL Polybrene in DMEM (10% FBS, antibiotic-free) was distributed to the wells, followed by the addition of the sacsin knockdown or the control lentiviral particles ($1{,}25x10^5$ particles/well, MOI = 0,1). After incubating for 48h, the medium was replaced by DMEM (10% FBS, 1%Pen/Strep). After 72h, cellular extracts were prepared for immunoblotting experiments.

3.8 Transfection and generation of *SACS* knockout clones

To generate *SACS* knockout cells, N/TERT-1 keratinocytes were transfected with CRISPR/Cas9 KO plasmids using jetPrime transfection reagent (Polyplus transfection, Illkirch, France), following the manufacturer´s instructions. Briefly, N/TERT-1 (Passage 7) were cultured in a 6-well plate in antibiotic-free K-SFM medium until reaching 70% confluency. On the day of transfection, 1µg/well of sacsin CRISPR/Cas9 KO plasmid was diluted in jetPrime transfection buffer (100 µl per µg of plasmid), and jetPrime transfection reagent plasmid was added (2µl/µg of plasmid). After incubating for 10 minutes at room temperature, the transfection mixture was added to the medium of the cell culture and incubated at 37ºC, 5% CO_2. After 72h, the medium was removed, and cells were detached using trypsin. After centrifugation, the pellet was resuspended in antibiotic-free K-SFM medium. Cells that were positive for GFP were selected using a FACS Aria III (BD Biosciences, San Jose, CA, USA), resulting in 144 GFP + individual clones. After sorting, the individual clones were cultured in K-SFM medium.

3.9 Microscopy and data analysis

Brightfield and fluorescence images were acquired in a Nikon TE2000-S microscope, equipped with an Evolution MP camera (Media Cybernetics Inc. Rockville, MD, USA), with Image-Pro-Plus v7.0 software (Media Cybernetics Inc. Rockville, MD, USA). To measure epidermal thickness, parallel sections of three independent experiments were stained with H&E and three different regions were imaged per section. Each image was measured three times using ImageJ 1.53e. Calculation of mean thickness values and standard error (SE) between triplicates and graphical representation was done using GraphPad Prism 9 (GraphPad Software, San Diego, California, USA).

Fluorescence quantification and immunoblot quantification was done using the gel plugin of ImageJ 1.53e. For each image, the lanes were selected, the intensity plotted as a curve, and the area under each curve was calculated. Each protein was normalized by calculating the ratio between each lane value and the corresponding lane of a housekeeping protein (GAPDH unless otherwise stated). Relative expression was done by dividing the normalized protein expression of each experimental group by a designated control group. Graphical representation and statistical calculation were done using GraphPad Prism 9. Statistical significance was calculated by one-way ANOVA, followed by Tukey's test. Significance was considered when $p<0.05$.

4 Results

4.1 HaCaT keratinocytes generate a 3D epidermal model without a stratified morphology

The HaCaT cell line[51] is a spontaneously immortalized human keratinocyte cell line extensively used in research. However, most studies focus on 2D cell culture approaches. We aimed at generating a novel 3D epidermal model using this cell line. First, we tested whether different cell culture media and the addition of supplements known to promote epidermal stratification and differentiation would affect epidermal morphology. The protocol followed was described previously in section 3.3. The different conditions tested and the resulting epidermal morphologies are detailed in Table 8.1 (Supplementary information). Using DMEM medium during all the steps of the protocol, which has calcium in its composition, did not allow the development of an epidermis. It was only observed 1-2 layers of cells with both cellular density values tested (Fig. 4.1A).

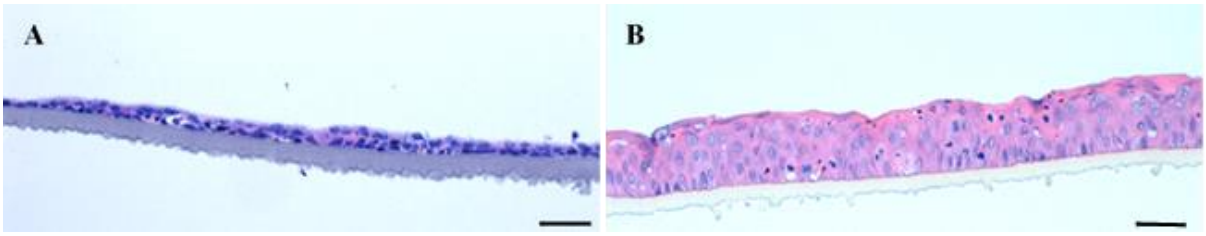

Figure 4.1 Comparison of the effect of different cell culture medium in epidermal morphology. Two different cell culture media were tested, DMEM (A) and Epilife (B), both supplemented with L-ascorbic acid and keratinocyte growth factor (KGF). Same seeding cellular density ($5x10^5$ cells/cm^2) and the same number of air-liquid interface days (14) were used. Epilife medium allows the supplementation of different calcium concentrations during different steps of the protocol stimulating the formation of multiple layers of cells. The images were taken with a magnification of 200x. Scale bar is 50µm.

When a calcium-free medium was used, allowing customized calcium supplementation to generate a steep increase in calcium concentration during epidermal formation (0,06mM during monolayer culture and 1,5mM after seeding in the polycarbonate layer), a more complex 3D cellular arrangement was observed (Fig. 4.1 B). Nonetheless, the epidermis generated did not present all the distinctive layers that comprise a native epidermis. One of the hallmarks of a fully differentiated epidermis is the presence of the *stratum corneum*, which did not form under any of the conditions tested. HaCaT cells have been described to be sensitive to different levels of calcium in the culture medium, with low levels being associated with a basal phenotype and high levels inducing a differentiated state[108,109]. Hence, promoting a basal phenotype by reducing the calcium concentration to very low levels in 2D culture prior to inducing 3D differentiation with a high calcium stimulus could promote better stratification. However, further reducing calcium concentration during cell culture (0,03mM) prior to seeding on the insert did not improve epidermal stratification (Supplementary Information Fig. 8.1).

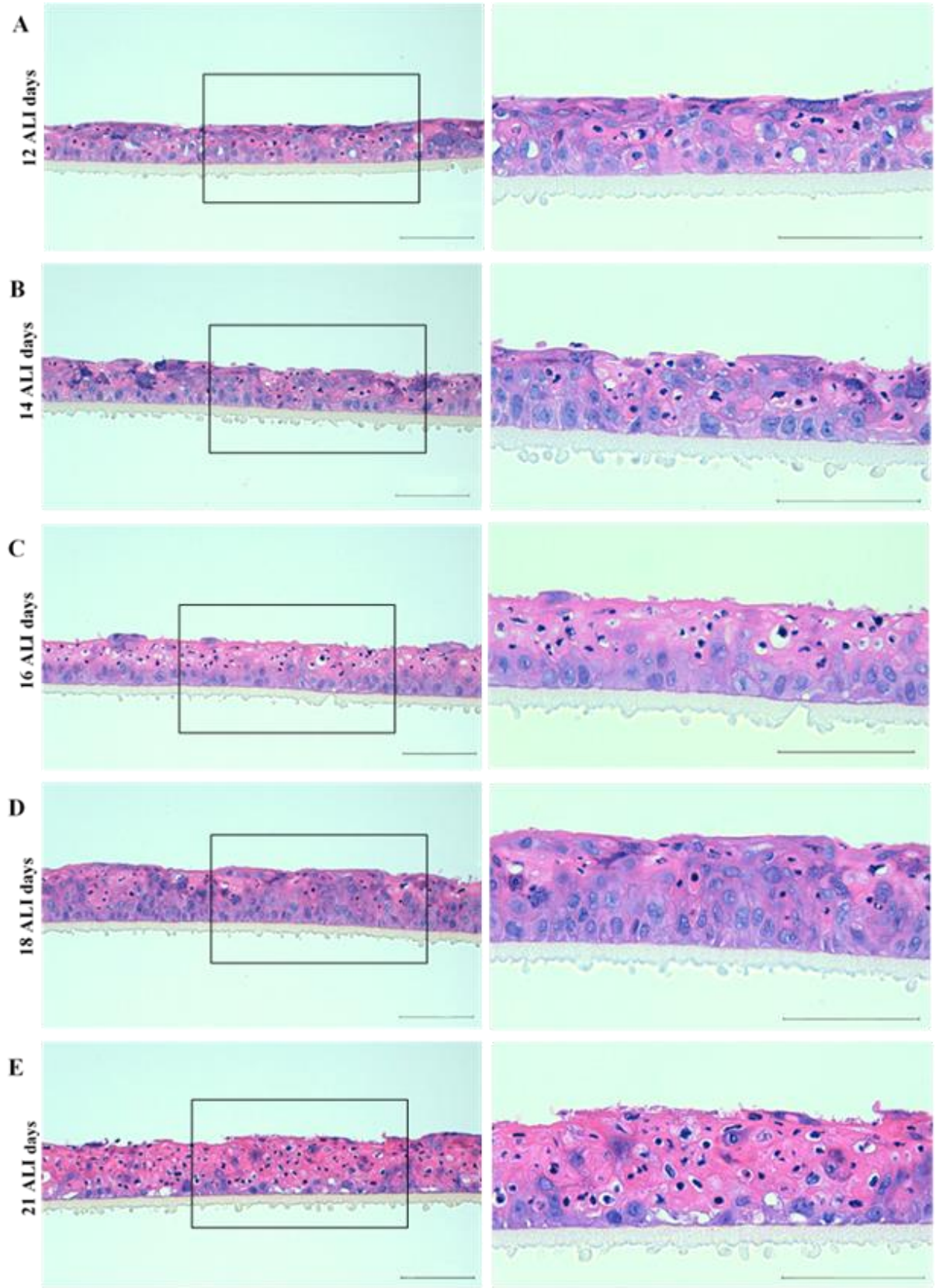

Figure 4.2 (A-K) Influence of ALI days on the HaCaT epidermal model. Different number of days (12, 14, 16, 18, 21, 23, 26, 28 and 31) of ALI conditions were tested using Epilife medium, supplemented with L-ascorbic acid and keratinocyte growth factor (KGF), with the same seeding cellular density ($5x10^5$ cells/cm^2). H&E staining of representative images (three independent experiments, n=3) of different ALI days (A, B, C D, E, F, G, H, I) are shown with two magnifications, 200x (left panel) and 400x (right panel). Representation of mean epidermal thickness as time progresses with SE (J). Measurements were done using three independent assays for each condition (N=3) and nine measurements per experiment. Cellular proliferation is shown by Ki67 staining (K) counterstained with hematoxylin. Scale bar in all images (A-I, K) is 100µm.

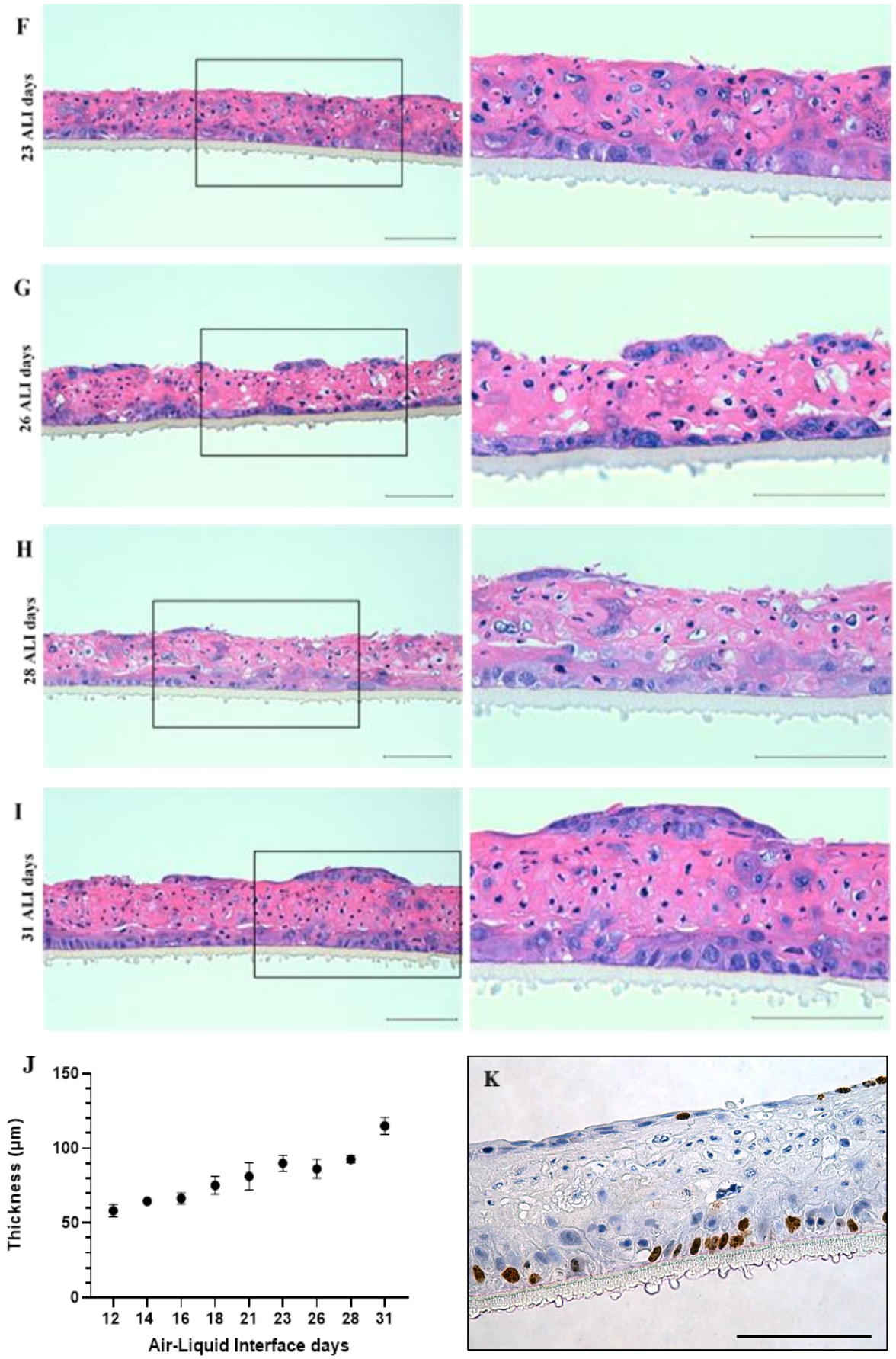
F
23 ALI days
G
26 ALI days
H
28 ALI days
I
31 ALI days
J
Thickness (µm)
150
100
50
0
12 14 16 18 21 23 26 28 31
Air-Liquid Interface days
K

We tested if increasing the number of days the epidermis was kept in air-liquid interface (ALI) conditions could promote the formation of the *stratum corneum*. In ALI, only the bottom of the insert is in contact with the medium, mimicking the natural process of epidermal formation. Up to 14 ALI days (Fig. 4.2 A, B), the epidermis showed a disorganized morphology, without any distinctive layers present. As time progressed (Fig 4.2 C, D), two separate layers became more evident: a basal layer, where the cells had a cuboidal shape and were spatially close to each other; and an upper layer where cells were more loosely packed and had a flatter appearance with smaller nuclei. With increasing ALI days, there was also an apparent growing disorganization in the overall cellular arrangement (Fig. 4.2 D-I), with a reduction of the so-called basal layer to a 1-2 cell layer located in the bottom of the epidermis (Fig. 4.2 E-I). At 26 ALI days, a discontinuous third layer appeared in the form of patches that had a similar cellular arrangement to that of the basal layer (Fig. 4.2 G, H, I). By increasing the time of ALI conditions, the overall thickness of the epidermis increased (Fig. 4.2J), mostly due to the increasing thickness of the upper layer. The maximum thickness (115µm) was achieved after 31 days of ALI. We also verified that after 31 days of ALI, the cells in the basal layer were still proliferating, as they were positive for Ki67 (Fig. 4.2 K).

4.2 The HaCaT epidermal model presents an incomplete epidermal differentiation phenotype

During the differentiation process from the *stratum basale* to the *stratum corneum*, keratinocytes express several different proteins that can be used as markers to evaluate epidermal maturation. To further characterize the HaCaT epidermal model, we assessed how the number of ALI days had an impact on the spatial expression of epidermal markers keratin 14 (K14), keratin 15 (K15), keratin 10 (K10), and involucrin (Inv). In normal human epidermis, there is a switch from expressing K14 to K10 as keratinocytes move from the basal layers to a more differentiated state in the upper layers [22,23]. Our results indicate that K14 was more expressed in the basal layer of the epidermis after 14 ALI days, but with some expression also in the upper layers (Fig. 4.3A). The fluorescence in the basal layer decreased as time progressed, but K14 expression was still mainly localized in the lower half of the epidermis (Fig. 4.3 B, C). Opposite to K14, keratin 10 (K10) expression was observed on the upper layers of the epidermis (Fig. 4.3 D, E, F), which is especially evident at 31 ALI days (Fig. 4.3 F).

Keratin 15 expression has been described in the basal layer of fetal epidermis and in the bulge of the hair follicle in adults. However, it is downregulated in keratinocytes in epidermal equivalents undergoing differentiation[110], being associated with an undifferentiated phenotype and stem cell-like properties [111,112]. We observed that K15 was still expressed at later ALI days (Fig. 4.3 H, I), suggesting that even after 31 ALI days HaCaT keratinocytes did not reach terminal differentiation.

Involucrin (Inv) is a precursor of the cornified envelope typically expressed in the *stratum corneum* and the *stratum spinosum*[113,114]. Involucrin expression was low at 14 ALI days (Fig. 4.3 J), but there was a slight increase with time (Fig. 4.3 K, L). However, involucrin was not localized in any particular region of the epidermis, revealing an incomplete epidermal maturation, as was also suggested by the absence of defined epidermal layers, especially the *stratum corneum*.

The fluorescence of each marker mentioned above was plotted with the number of ALI days (Supplementary information Fig. 8.2). K14 expression was stable during the 31 days in ALI conditions, with a slightly lower value at 23 ALI days. K10 and Inv had a low expression at 14 days ALI, but then expression increased until it reached a peak at 31 days ALI for both K10 and Inv. K15 expression increased until 23 ALI days, reaching a very low level after 31 ALI days. Even though K14 remained stable with time, these results suggest that there was an increase in the expression of markers associated with epidermal differentiation with increasing ALI days and a decrease of cells with an undifferentiated

phenotype. However, these results should be seen with caution, as only a low number of replicates were used. In addition, these results refer to the expression of each marker in the entire epidermis, not on specific layers, which does not allow to follow how the expression of each marker evolved on a particular layer.

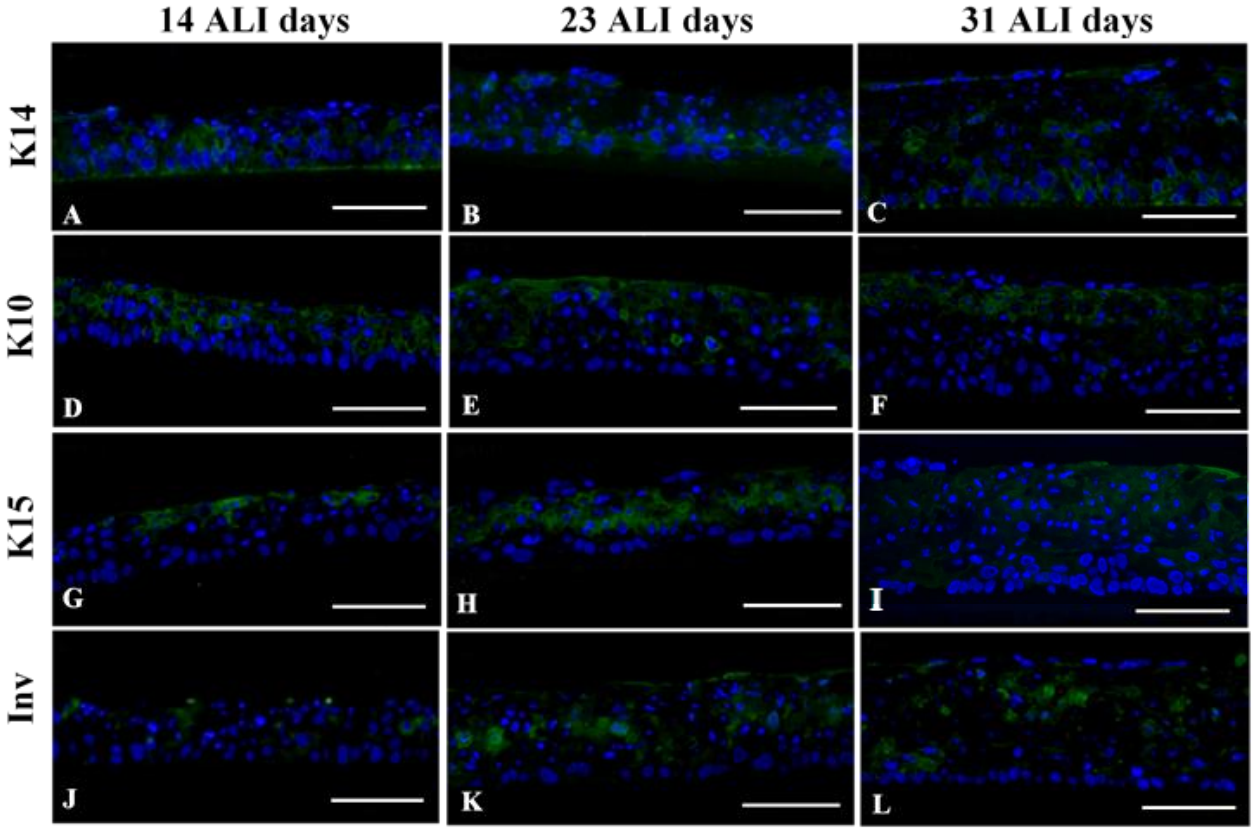

Figure 4.3 (A-L): Expression of epidermal markers in the HaCaT cell model at different ALI days. Representative images showing the expression of keratin 14 (K14, A, B, C), keratin 10 (K10, D, E, F), keratin 15 (K15, G, H, I) and involucrin (Inv, J, K, L), stained green, at 14, 23 and 31 ALI days. Nuclei are stained with DAPI (blue). Although the localization of the markers is disperse within the epidermis, K14 (A-C) and K10 (D-F) expression was mainly located in the lower part and upper layers of the epidermis, respectively. K15 expression was visible throughout the time of the experience (31 ALI days) (G-I) and Inv (J-L) was not localized in the outer layers of the epidermis, pointing to insufficient differentiation and maturation. Images were taken with a magnification of 400x. Scale bar in all images (A-L) is 100µm.

4.3 N/TERT-1 epidermal model recapitulates native epidermal characteristics

After observing that the HaCaT cell line was unable to generate a fully differentiated epidermis, we tried to establish a new epidermal model using the N/TERT-1 cell line. This is a keratinocyte cell line immortalized by expression of human telomerase reverse transcriptase (hTERT) and loss of the pRB/p16^{INK4a} cell cycle control mechanism, first established by Dickson et al. [105]. This cell line has been successfully used to produce human epidermal equivalents with similar characteristics to those generated using primary keratinocytes[58,59,115,116]. To promote cellular adhesion to the scaffolds, a few changes had to be made to the protocol developed to generate the epidermal equivalents for the HaCaT cell line. The first modification was the coating of the scaffolds with collagen type I before seeding the keratinocytes. The second alteration was the addition of a longer submerged phase before raising the inserts to ALI conditions (Fig. 3.2).

The ideal cell density to generate a model with a multi-layer morphology, similar to human epidermis, was $3x10^5$ cells/cm^2 and the lowest number of ALI days needed to promote stratification was 14 (Fig. 4.4A). Increasing the cell density in the insert did not improve morphology or the thickness of the epidermis (Supplementary information Fig. 8.3). We observed the different *strata* that characterize a fully differentiated epidermis (Fig. 4.4 A). The *stratum basale* could be identified in the lowest layer of cuboidal-shaped cells that are tightly packed together and highly proliferative, as indicated by the expression of the proliferation marker Ki67 (Fig. 4.4 B). The *stratum spinosum* can also be distinguished, where cells showed a more elongated shape. Above them, the *stratum granulosum* was characterized by the appearance of granules inside the cells. Contrary to what was observed in the HaCaT epidermal model, here we could observe the formation of the *stratum corneum*, which indicates the presence of the last stage of the epidermal maturation process.

Similar to the HaCaT model, we used immunofluorescence to evaluate the expression of different epidermal markers. K14 expression was limited to the basal layer of the epidermis (Fig. 4.4 C). K15 expression was very low throughout the entire epidermis (Fig. 4.4 D), as expected for a fully differentiated epidermis. Involucrin expression was observed mainly in the outermost layers, specifically in the *stratum granulosum* (Fig. 4.4 E). K10 was expressed in the upper layers, but not in the basal layer (Fig 4.4 F). From the results obtained by morphological assessment and specific differentiation marker expression, we can conclude that the N/TERT-1 cell line can generate an epidermal model with characteristics of native human epidermis.

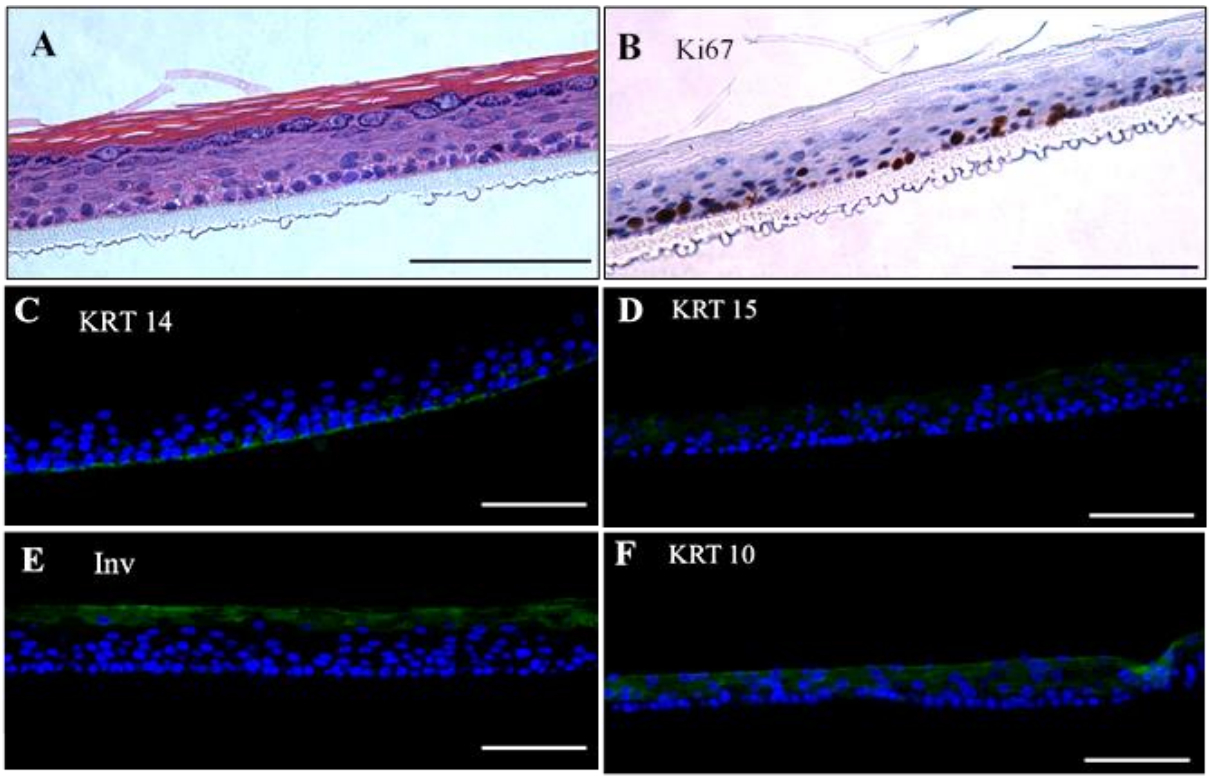

Figure 4.4 (A-F) Characterization of the N/TERT-1 epidermal model. Multi-layer architecture is visible with H&E stain (A). Cellular proliferation in the basal layer is shown by Ki67 staining (B) counterstained with hematoxylin. Expression of K14 (C), K15(D), Inv(E) and K10 (F) are shown in in green, nuclei are stained with DAPI (blue). K14 was expressed in the basal layer (C) while K15 had a low expression in the epidermis (D). Inv (E) and K10 (F) were expressed in the top layers of the epidermal model. Representative images of three independent experiments (n=3) are shown with different magnifications (A, B with 400x and C, D, E and F with 200x). Scale bar represents 100µm in all images.

4.4 HaCaT keratinocytes express low levels of the sacsin protein

Epidermal models can be important tools in understanding the molecular mechanisms underlying disease and can potentially foster the development of therapeutics, by mimicking *in vitro* the disease phenotype. We aimed at generating an epidermal model that replicates the ARSACS skin phenotype by ablating sacsin function[102]. We started by analyzing the expression of sacsin in the HaCaT cell line in two different passages (P.52 and P.62) versus human epidermal keratinocytes (HEK), the rat glioma cell line C6 (positive control) and a C6 *SACS* KO cell line (negative control, previously generated by Fernanda Murtinheira at Dr. Herrera's laboratory using a CRISPR/Cas9 approach to knockout the *SACS* gene) (Fig. 4.5 A). As expected, sacsin was highly expressed in the C6 cell line and no band was observed in the C6 *SACS* KO cell line. Regarding the keratinocytes, HEK had much lower expression than C6 cells (0,074±0,0350), but similar to HaCaT cells. Both HaCaT passages showed very low levels of sacsin expression relative to C6, both below 0.1 (HaCaT P52: 0,011±0,001, HaCaT P62: 0,085±0,064) (Fig. 4.5 B). The difference of sacsin expression between C6 and all the keratinocytes was found statistically significant, but no statistical significance was observed between either the different HaCaT passages, or between these and HEK (One way ANOVA, $p<0.05$). Therefore, we concluded that sacsin was expressed in similar amounts in HaCaT cells and HEK, despite being low relative to C6 cells.

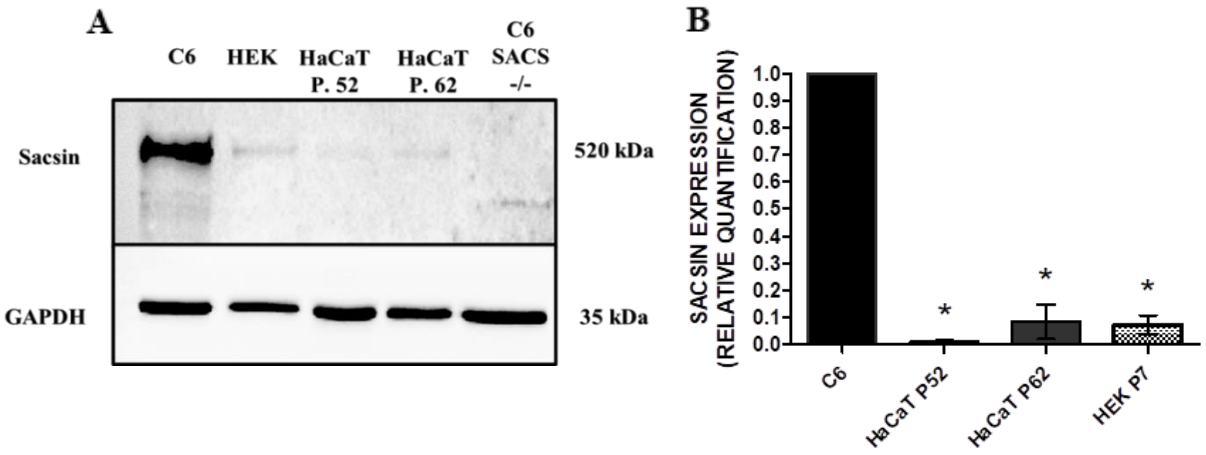

Figure 4.5 (A, B) Expression of sacsin in HaCaT keratinocytes. Sacsin expression in C6 cell line, human epidermal keratinocytes (HEK), two passages of the HaCaT cell line (P52, P62) and C6 *SACS* KO cells (C6 *SACS* -/-) as a negative control was analyzed by immunoblotting. A band corresponding to sacsin at 520 kDa is present with different intensities and is visible in all cell types analyzed, except on the negative control (C6 *SACS* -/-). Glyceraldehyde 3-phosphate dehydrogenase (GAPDH) was used as a loading control in all samples. Both HaCaT passages (P.52 and P.62) and HEK have similar sacsin expression, but keratinocyte express low levels when compared with C6 cell line (B). Sacsin quantification was done using 2 independent experiments (N=2), sacsin expression was normalized to GAPDH expression and is relative to C6. Bars show mean± SE. Statistical analysis was done using One way ANOVA. *, significant vs C6, $p<0.05$.

Since the HaCaT cell line expressed sacsin, we tried to knockdown its expression by lentiviral transduction using vector-based short hairpin RNAs (shRNAs). Immunoblotting to confirm sacsin deletion revealed the absence of a sacsin band in HaCaT cells that were transduced, but also in the non-transduced control (Fig. 4.6). The inability to confirm sacsin expression in the control group did not allow us to conclude whether the absence of sacsin in the shRNA-treated group was a result of the conducted experiment or simply because sacsin expression was very low in the particular HaCaT subpopulation used to conduct this experiment. Nevertheless, this result further supports that sacsin expression is very low in HaCaT cells, so a different approach is needed to develop an epidermal model with an ARSACS phenotype.

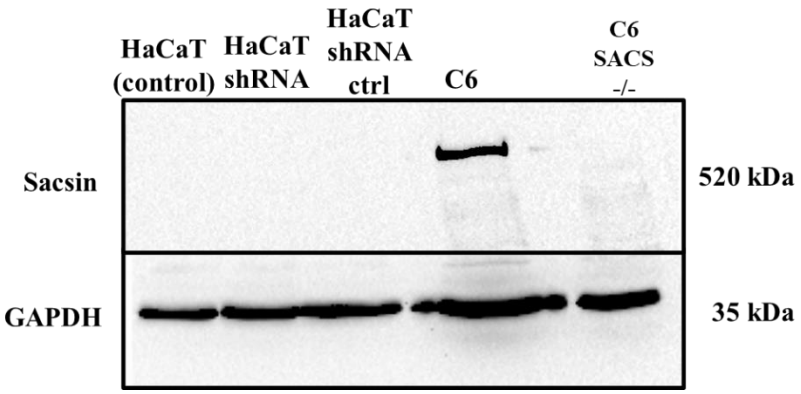

Figure 4.6 Sacsin expression after knockdown using lentiviral transduction. Sacsin expression was analyzed by immunoblotting in non-transduced HaCaT (control), HaCaT transduced with shRNA (HaCaT shRNA), and HaCaT transduced with control lentiviral particles (HaCaT shRNA ctrl). C6 cell line was used as a positive control and C6 *SACS* KO cells (C6 *SACS* -/-) as a negative control. A band corresponding to sacsin at 520 kDa is present in C6 cells, but absent on the remaining experimental groups, including the HaCaT control group. Glyceraldehyde 3-phosphate dehydrogenase (GAPDH) was used as a loading control and a band corresponding to this protein is visible in all samples.

4.5 Sacsin is differentially expressed in skin cells

Sacsin is expressed in most tissues although at different levels, according to the Human Protein Atlas (available from http://www.proteinatlas.org)[94,95]. Fibroblasts have already been used in previous ARSACS studies[96,103], but sacsin expression and function remain elusive in the skin. Since our previous results indicated that HaCaT keratinocytes express low levels of sacsin, N/TERT-1 keratinocytes were tested to establish the best approach to generate an ARSACS skin model and better characterize sacsin expression in different skin cells.

Two different antibodies, one against N-terminal (aminoacids 787 to 809) and the other against the C-terminal were used to compare the different expression profiles of sacsin in the different cell types (Fig. 4.7). Both antibodies stained a high molecular weight band (520 kDa) that likely corresponds to full-size sacsin (Fig. 4.7 A, B). Moreover, bands with a lower molecular weight were also present with both antibodies, which can be smaller truncated forms of sacsin or due to unspecific staining. To compare the different sacsin levels, the intensity of the high MW band (520 kDa) was quantified and represented as a fraction of the value obtained for C6 cells (positive control for high sacsin expression) (Fig. 4.7 C, D). Quantification (relative to C6 expression) of the 520 kDa band using the N-terminal antibody revealed that human dermal fibroblasts (HDFn) expressed the most sacsin (0,44) after C6 cells (Fig. 4.7 C). Both keratinocytes (HEK and N/TERT-1) expressed the lowest levels of sacsin. HEK sacsin expression was 0.10 relative to C6, while in N/TERT-1 keratinocytes was about 0.03, indicating a slight difference in sacsin expression between them.

Using an antibody that stains the C-terminal of the sacsin protein, we observed more intense bands in the 520 kDa region for all cell types. The main difference in sacsin expression when compared with the N-terminal staining antibody was observed in HEK (Fig. 4.7 B). Relative quantification showed that full-size sacsin in HEK had a higher expression (0,55) than HDFn (0,45) and N/TERT-1 (0,11). Similar to what was observed in the results obtained from the N-terminal antibody, N/TERT-1 keratinocytes were the cells that expressed the least sacsin but had a higher expression relative to C6 than in the previous results. Considering that the band in C6 cells did not appear to have lower intensity using the C-terminal versus the N-terminal antibody (Fig. 4.7 A, B), but the opposite, we cannot conclude that the higher value in N/TERT-1 was due to a lower sacsin expression in C6 cells. In addition to the fact that N/TERT-1 expressed sacsin, HEK (using the C-terminal antibody) and HDFn showed high sacsin expression (which suggests that an ARSACS skin model could be relevant to study sacsin function.

Below 520kDa, bands and their intensity varied, but there was a similar band profile in the skin cells (N/TERT-1, HEK and HDFn). Further studies are needed to clarify sacsin expression in keratinocytes, especially N/TERT-1, and to try to understand if these bands are truncated sacsin forms or not.

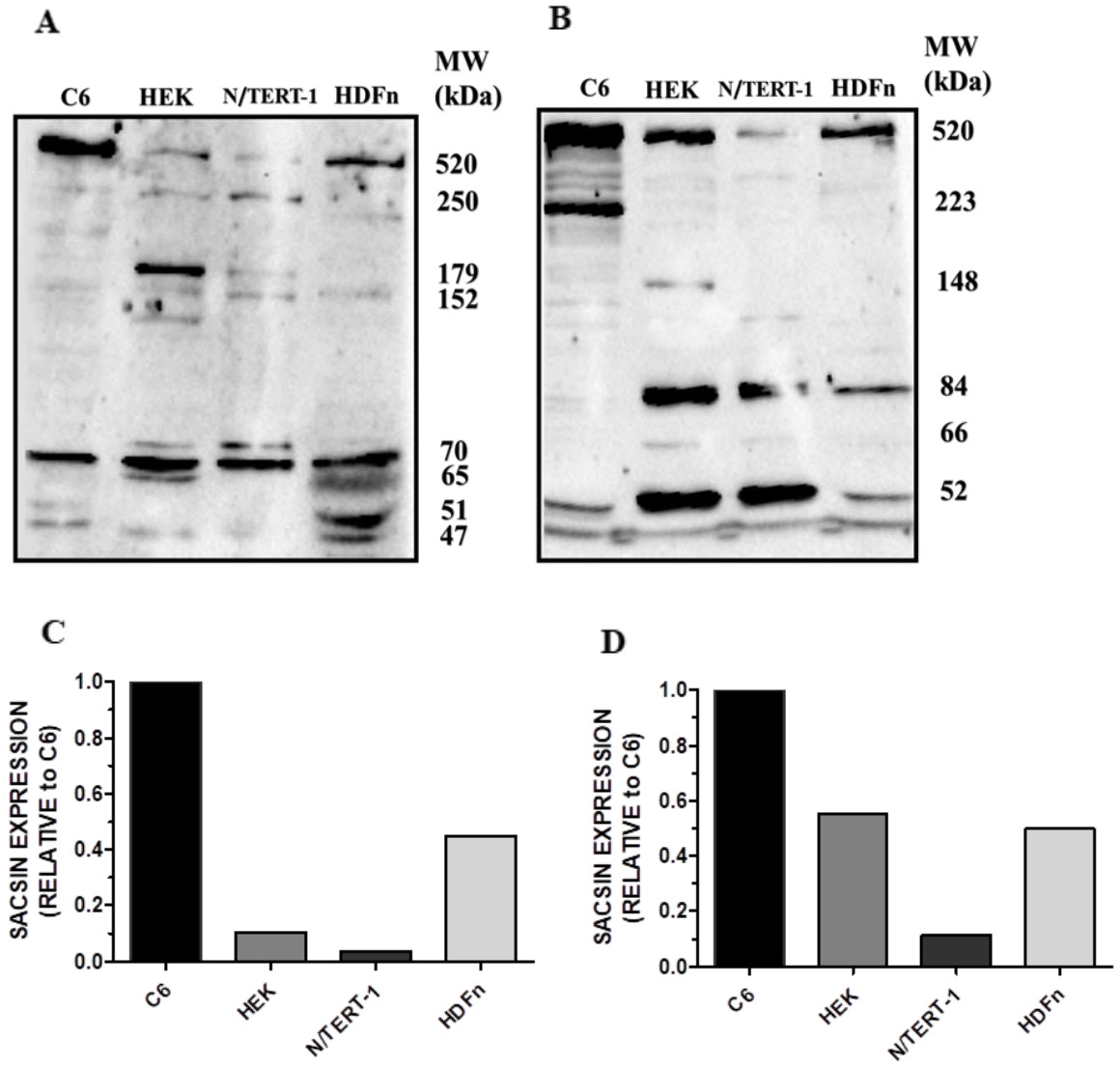

Figure 4.7 (A-D) Sacsin expression in skin cells. Sacsin expression was analyzed in C6 cells, human epidermal keratinocytes (HEK), N/TERT-1 keratinocytes and human dermal fibroblasts (HDFn) by immunoblotting using two different antibodies: one against N-terminal (A, C) and other against the C-terminal (B, D). Different bands are visible depending on the antibody used, but a high molecular heigh band corresponding to full-size sacsin is common to both antibodies (A, B). Sacsin quantification was done using the blots shown, and it is relative to C6 expression (C, D). Each well was loaded with 35µg of total protein.

5 Discussion

The skin constitutes a functional barrier that separates the organism from the outside environment, maintaining homeostasis. Two main layers (the dermis and the epidermis) make the skin a complex three-dimensional structure capable of protecting the body from external stressors. Due to growing pressure to reduce animal usage in research and industry, the demand for the development of *in vitro* 3D skin models has been increasing in recent years. These allow the recreation of native skin architecture, and they can also be tailored to meet the needs of different fields. ARSACS is a rare disease that is mainly characterized by spasticity and lack of coordination of muscle movements [64,66,68], but skin abnormalities have also been reported in ARSACS patients[74], making this disease an interesting candidate to study using 3D skin models. Mitochondrial dysfunction[96,97,99,100] and anomalies in the organization of the IF structure[102–104] have been associated with defective sacsin function, but a comprehensive overview of this protein is still lacking. To further expand the current knowledge of sacsin, in this project we developed and characterized novel 3D epidermal models to explore the role of this protein in the human skin.

In this work, two reconstructed human epidermal models were developed using different human keratinocyte cell lines, the HaCaT cell line, a spontaneously immortalized cell line[51], and the N/TERT-1 cell line, which consists of hTERT-immortalized keratinocytes[105]. The HaCaT cell line is broadly used in research, although mainly in 2D culture. Here, we established a novel human epidermal model using a commercially available scaffold to seed the keratinocytes. First, we studied how different culture conditions affected the development of the HaCaT epidermal model. Two media compositions were tested, Epilife and DMEM, only the former allowing the generation of different calcium concentrations during epidermal development, because it has no calcium in its composition. DMEM already has calcium in its composition, therefore not enabling keratinocyte 2D culture with low calcium levels. Epidermal differentiation was absent when DMEM was used, thus suggesting that calcium might play an important role in HaCaT differentiation (Fig. 4.1). Calcium has been reported to regulate the transcription of genes associated with epidermal differentiation in HaCaT, such as keratin 1 (K1), plasminogen activator inhibitor type 2 (PAI-2), and involucrin (Inv)[109,117]. PAI-2 and involucrin are associated with the cornified envelope formation[118], while K1 is a type II intermediate filament mostly expressed in the upper epidermal layers[23]. This differentiated phenotype will probably result in a reduced proliferation activity that will not allow the formation of a functional basal layer, from which all the upper layers derive. Another advantage of using Epilife medium instead of DMEM is the absence of FBS supplementation, which has an undefined and variable composition that can contribute to decreased reproducibility between assays. Recently, serum lipids have been found to suppress K1/K10 expression in HaCaT and primary keratinocytes in 3D cultures, possibly due to the presence of retinoids[119]. This suggests an alternative way of inhibiting epidermal formation by the inhibition of HaCaT terminal differentiation.

Despite still containing low amounts of undefined products, such as BPE and bovine transferrin, Epilife has a mostly defined composition of the different factors used to promote keratinocyte growth. One of these factors that can play an important part in improving HaCaT stratification is EGF since it has been demonstrated that it upregulates KGF receptors, otherwise little expressed in HaCaT cells[54]. KGF plays an important role in wound repair, proliferation and differentiation of keratinocytes[120,121], and previous studies have shown that it can also improve HaCaT epidermal stratification[54]. Although the HaCaT epidermal model developed in this work presented some degree of differentiation, the strata that are characteristic of normal human epidermal morphology were not present. From 16 days ALI onward, two layers become more evident: a basal layer that resembles the *stratum basale* of native epidermis and the upper layer where cells are disorganized and loosely packed (Fig. 4.2). Despite an

increase in epidermal thickness as the number of ALI days increased, there was no formation of the *stratum corneum* after 31 days of ALI conditions. Its morphology shared some features with parakeratotic epithelia, mainly characterized by the presence of nuclei in the outermost layers due to incomplete keratinocyte differentiation. Parakeratosis is usually associated with more benign skin diseases, such as dermatitis, but has also been associated with squamous cell carcinoma[122,123]. Although not tumorogenic, the HaCaT cell line exhibits a transformed phenotype and chromosomal anomalies[51] which may be the underlying cause of this inefficient stratification. Previous studies have attempted to build a 3D epidermis using HaCaT keratinocytes with insufficient stratification and differentiation and the absence of the *stratum corneum*[52–55,124,125]. Up to this day, the HaCaT cell line only showed similar differentiation and stratification to primary keratinocytes after *in vivo* transplantation into nude mice[51,126]. One explanation might be that mechanical stimuli play an important part in HaCaT epidermis differentiation and keratinization. It was reported the formation of the *stratum corneum* and the upregulation of terminal differentiation markers (involucrin and filaggrin) *in vitro* by using a device that allows both air exposure and mechanical stimulation[56]. Although the HaCaT cell line may not be the best candidate to produce a 3D model that mimics the human epidermal architecture, in this work we developed a novel HaCaT epidermal model using a commercially available inert polycarbonate membrane, in contrast to the majority of the previous models that use either a collagen matrix[52–54,124,125] or a fibroblast-derived dermal equivalent[55]. Further attempts at developing a HaCaT epidermal model should probably consider combining mechanical stimulation to the parameters optimized in this work for optimal epidermal maturation.

The N/TERT-1 cell line, on the contrary, is a cell line that is not as extensively studied as the HaCaT cell line, but it has demonstrated a differentiation capacity similar to human primary keratinocytes in three-dimensional cultures[58,59,115,116,127,128]. Here, we further supported those results by showing that this cell line can form a fully differentiated epidermis *in vitro*, with all the *strata* normally present in native human skin (Fig. 4.4 A). Importantly, the *stratum granulosum* (the last *stratum* before the *stratum corneum* characterized by cells with multiple granules) is present in our model, which is often not formed or scarce in many previously published skin models using the N/TERT-1 cell line[115,116]. Additionally, in our N/TERT-1 model, all the layers are distinguishable: the *stratum basale*, where cuboidal shaped cells are tightly packed together and responsible for keratinocyte proliferation (showed by Ki67 staining, Fig. 4.4 B), which then move upwardly as they differentiate; the *stratum spinosum* where the cells showed a more elongated shape, the *stratum granulosum*, and the *stratum corneum*. The *stratum corneum* is a hallmark of epidermal differentiation and it is an important determinant in barrier formation and surface permeability[129]. A previous study has shown that N/TERT-1 skin models have comparable permeability to that of primary keratinocytes skin models[116], but further studies are needed to validate these results and to extend their applications. Finally, we have also demonstrated that the supplements (KGF, L-ascorbic acid, and calcium) used to promote epidermal stratification in primary keratinocytes[16] can also have the same effect on the N/TERT-1 cell line.

Keratinocyte progressive maturation as they move from the *stratum basale* to *the stratum corneum*, where they reach terminal differentiation, is accompanied by the expression of different keratins[22,23]. We used four epidermal differentiation markers (K10, K14, K15, and involucrin) to better characterize the epidermal development of the HaCaT epidermal model as time progressed (Fig. 4.3) and to validate the N/TERT-1 epidermal model (Fig. 4.4 C-F). Keratin 14 (K14) expression in the HaCaT model was higher in the basal layer of the epidermis after 14 ALI days, decreasing as time progressed, but K14 expression was also visible in the top layers. On The N/TERT-1 model expression of K14 was restricted to the basal layer of the epidermis, as it has been described for native human epidermis and epidermal models using primary keratinocytes[16]. K10 was expressed on both models in the upper epidermal layers, but not on the basal layer. Involucrin expression, which is in addition to K10

another marker of keratinocyte differentiation, was low in the HaCaT model but it was visible in the *stratum granulosum* in the N/TERT-1 model.

Suprabasal expression of K10 on both models was comparable to what has been described for other epidermal models using N/TERT-1[59,116,127] and primary human keratinocytes[16]. The same expression pattern is in accordance with native human skin[16,130]. Involucrin is a protein expressed in the cytoplasm of keratinocytes in the later stages of differentiation, mainly in the *stratum spinosum* and *granulosum*, that is then integrated into the cornified envelope, forming the *stratum corneum*[113]. Our results in the N-TERT1 model reproduce the involucrin-positive immunostaining on the upper part of the *stratum spinosum* and the *stratum granulosum* observed in normal human skin and other N/TERT-1 epidermal models[59,131]. A similar expression of K10 and disperse localization of Inv and K14 have been previously reported in organotypic coculture systems using HaCaT keratinocytes in collagen matrix embedded with fibroblasts [52,119,125]. The abnormal expression of these epidermal markers in the HaCaT model may be another consequence of this cell line transformed phenotype since K14 overexpression in the upper epidermal layers is a common feature in squamous cell carcinomas and K14 depletion was shown to reduce tumorigenicity[132,133]. Moreover, downregulation of K14 induced the expression of differentiation markers, such as involucrin[133], suggesting that maybe the overexpression of K14 in our HaCaT model could be contributing to the inhibition of involucrin expression. K15 is a minor type I keratin expressed with the most abundant pair K5/K14 in the basal layer of human epidermis[134]. Contrary to what was observed in adults where K15 is expressed in patches in the basal layer, in neonatal epidermis and up to the age of 1,5 years its expression is uniform throughout the *stratum basale*[110,135], therefore pointing to a possible role of K15 in developing epidermis. K15 has been suggested as an epidermal stem-cell marker in the hair follicle[111,112] and it is overexpressed in basal cell carcinomas (BCC)[134], but downregulated in keratinocytes in epidermal equivalents undergoing differentiation[110]. This evidence points to a K15 being an indicator of an undifferentiated state in the epidermis. Therefore, K15 expression in the HaCaT model throughout the epidermal layers but not in the N/TERT-1 model, may be another indicator that HaCaT keratinocytes are not fully differentiated, in contrast to the N/TERT-1 model.

The N/TERT-1 model developed here has the potential to be used in disease modeling and drug testing, as it has similar morphology and expression of K10 to commercially available *in vitro* skin models EpiDerm (MatTek, Ashland, MA, USA) and Episkin (L´Oreal; SkinEthic, Nice, France)[136]. Apart from its reproducibility and tailoring to specific needs, another advantage of our model over EpiDerm and Episkin is the expression of involucrin only in the *stratum granulosum* and *spinosum*, while in these models involucrin expression is visible in all suprabasal *strata*[136]. Despite the efforts to optimize the HaCaT epidermal model by varying the culture conditions and extending the number of ALI days, our results clearly indicate that the N/TERT-1 model mimics better native epidermal morphology and differentiation. In the future, permeability studies and in-depth expression studies should be performed to understand if this model has a comparable profile to human epidermis.

ARSACS is a rare, early-onset debilitating disease to which there is still no therapy available[68]. It is caused by the loss of function of sacsin, a multi-domain 520 kDa protein whose structure suggests a chaperone-like fuction[86–88]. Most research in ARSACS and sacsin function focuses on the central nervous system since the majority of ARSACS symptoms arise from the degeneration of Purkinje neurons in the cerebellum[72]. However, anomalies in skin biopsies of ARSACS patients have been reported[74], so the generation of an ARSACS skin model could provide more insights on sacsin function. For this purpose, we analyzed the expression of sacsin in multiple skin cells: HaCaT keratinocytes, N/TERT-1 keratinocytes, human primary keratinocytes (HEK), and human dermal fibroblasts (HDFn).

HaCaT cells expressed similar sacsin levels to HEK keratinocytes, but the expression was low when compared with C6 cells (Fig. 4.5). Previous sacsin expression studies were conducted in multiple cells by Fernanda Murtinheira (Dr. Herrera's laboratory) and high levels of expression were observed in C6

cells (unpublished work), thus they were used in this work as a positive control for high sacsin expression. A small increase in sacsin expression was observed in later-passage HaCaT cells (HaCaT P.62 Fig. 4.5B), but no statistical significance was observed between the relative expression levels of different passages. We tried to decrease sacsin expression by lentiviral transduction using vector-based short hairpin RNAs (shRNAs), but sacsin expression was absent in both the HaCaT cells that were transduced and in the non-transduced control (Fig. 4.6). The absence of sacsin expression in the HaCaT control group (not treated with lentiviral particles) could be a consequence of the smaller cellular population used to conduct the transduction experiment. If we consider the possibility that sacsin expression in HaCaT was restricted to a small percentage of cells in culture, when the number of cells used was reduced, the small amounts of sacsin expression could be so low that the threshold for sacsin detection by immunoblotting was not reached. Moreover, polybrene, used to enhance cellular infection by the lentiviral particles, can be toxic to cells and further reduce the number of cells after treatment, thus exacerbating the effect mentioned. In conclusion, the fact that sacsin expression in HaCaT keratinocytes is low and inconsistent, in addition to the sub-optimal epidermal differentiation *in vitro*, does not make this cell line a good option to develop an ARSACS epidermal model.

To better characterize sacsin expression in N/TERT-1, HEK and HDFn, two antibodies (one against N-terminal and one against the C-terminal) were used (Fig. 4.7). Both antibodies stained a high molecular weight band (520 kDa) that very likely corresponds to functional, full-size sacsin, as it is present in wild type C6 but not in the corresponding knockout cell line. The lower MW bands observed (probably truncated forms of the sacsin protein or unspecific bands) were different between antibodies and their intensities varied between cell types. Quantification of the 520 kDa band revealed that HDFn and HEK expressed higher levels of sacsin, with the N-terminal and C-terminal antibodies, respectively. N/TERT-1 cells expressed the lowest levels of sacsin in both experiments, but when the C-terminal antibody was used, sacsin expression was higher (relative to C6). The intensity of the 520 kDa band was overall higher with this antibody, which could indicate that the C-terminal antibody probably has a higher affinity to sacsin as it is a polyclonal antibody, in contrast to the N-terminal antibody that is monoclonal. The fact that sacsin expression in HEK was very different between experiments (including the results observed in Fig. 4.5), suggests that further experiments are needed to assess sacsin expression. Nevertheless, the fact that all these cell lines express full-size sacsin, especially the N/TERT-1 keratinocytes, is a favorable result that supports the development of an ARSACS skin model.

According to the Human Protein Atlas database [94,95], data obtained from immunological staining indicates that sacsin has a low expression in human skin (keratinocytes, fibroblasts, melanocytes and Langerhans cells were included in the analysis). The experiments conducted in this work may suggest otherwise, especially regarding fibroblasts, which were the cells with the most consistent results with both antibodies (relative sacsin expression was around 0,5 relative to C6 in both cases). Previous studies showed that fibroblasts expressed sacsin[96] and further studies carried out in fibroblasts from ARSACS patients showed the presence of hyperfused mitochondria and bundles of vimentin filaments[96,103], results in accordance with observations made in neurons due to sacsin loss-of-function[96,102–104]. Together with our results, these findings suggest that skin cells are also a model to consider when studying sacsin.

The lower MW bands could be truncated forms of the sacsin protein (because of degradation or alternative sequences) or due to unspecific antibody staining. Two low MW splice variants were submitted to the Uniprot database[137] (B2REB0_HUMAN; H0Y6M8_HUMAN), with 84 kDa and 93.9 kDa, respectively (data unreviewed by UniProtKB curators). A high-intensity band is visible at 84 kDa in the immunoblot using the C-terminal antibody in all skin cells, so there is a small possibility that this band corresponds to a splice variant. Further work needs to be done to characterize the function and activity of these smaller truncated sacsin forms, which could provide more insight into sacsin function on the skin.

Efforts in generating *SACS* knockout clones were done as described in section 3.8 of the Materials and Methods chapter. We attempted to knockout sacsin expression in N/TERT-1 keratinocytes using CRISPR/Cas9 technology and after optimizing some steps, 144 GFP+ clones were generated after sorting. Unfortunately, due to unforeseen circumstances, such as cell culture room contaminations and all the work constraints caused by the COVID-19 pandemic during 2020 and 2021, no further progress was made in this line of work. It is also important to point out that the COVID-19 pandemic had a big impact on the course of the experimental work presented here, not only due to the reduction of presential lab work but also derived from delays in critical material and reagents deliveries, and restricted access to equipment. These limitations were the main cause for the lack of multiple independent experiments for some sets of results and led to the inability to fulfill all the objectives initially proposed for this project. The next steps after sorting the N/TERT-1 *SACS* knockout clones would be clone expansion and confirmation of *SACS* gene deletion and the absence of sacsin expression. Selected clones would then be used to develop an epidermis using the protocol optimized for the N/TERT-1 model. Characterization of this new model would be focused on lipofuscin and IFs organization (in this case keratins), as alterations in these elements would be probable according to the literature[102–104]. Altogether, this project contributed to the creation of new epidermal models using keratinocyte cell lines, had a critical contribution in the creation of a new line of research and established the foundation for the development of an ARSACS skin model.

6 Conclusions

In this work, culture conditions were optimized to generate 3D reconstructed epidermal models, using a commercially available polycarbonate inert matrix as a substrate. The differentiation and stratification capacity of two keratinocyte cell lines, HaCaT and N/TERT-1, were studied to understand if they could be used to develop a 3D epidermis *in vitro*. Sacsin expression studies were conducted in skin cells as a first approach towards the development of an ARSACS skin model.

The HaCaT cell line demonstrated limited stratification capacity, without the normal *strata* present in native epidermis, and an aberrant expression of differentiation epidermal markers even after extending the air-liquid culture period up to 31 days. N/TERT-1 keratinocytes were able to mimic normal epidermal morphology, with all the layers present and comparable expression of keratins (K10, K14 and K15) and involucrin.

Sacsin was little expressed in HaCaT keratinocytes and full-size sacsin was variably expressed in skin cells. Our studies suggest higher expression of sacsin in primary keratinocytes (HEK) and primary fibroblasts (HDFn) than in N/TERT-1 keratinocytes. The fact that N/TERT-1 cells express full-size sacsin and they can mimic human epidermis in 3D culture, makes them ideal to use in future studies towards the creation of an ARSACS skin model.

7 References

1. Losquadro, W. D. Anatomy of the Skin and the Pathogenesis of Nonmelanoma Skin Cancer. *Facial Plast. Surg. Clin. North Am.* 25, 283–289 (2017).
2. Dale, B. A., Lonsdale-Eccles, J. D. & Holbrook, K. A. Stratum corneum basic protein: an interfilamentous matrix protein of epidermal keratin. *Curr. Probl. Dermatol.* 10, 311–325 (1980).
3. Sibrack, L. A., Gray, R. H. & Bernstein, I. A. Localization of the histidine-rich protein in keratohyalin: a morphologic and macromolecular marker in epidermal differentiation. *J. Invest. Dermatol.* 62, 394–405 (1974).
4. Rothman, S. Keratinization in Historical Perspective. in *The Epidermis* (eds. Mntagna, W. & Lobitz, W.) 1–14 (Academic Press, 1964). doi:https://doi.org/10.1016/B978-1-4832-3293-5.50007-3
5. Menon, G. K., Cleary, G. W. & Lane, M. E. The structure and function of the stratum corneum. *Int. J. Pharm.* 435, 3–9 (2012).
6. Mathes, S. H., Ruffner, H. & Graf-Hausner, U. The use of skin models in drug development. *Adv. Drug Deliv. Rev.* 69–70, 81–102 (2014).
7. Odland, G. F. A submicroscopic granular component in human epidermis. *J. Invest. Dermatol.* 34, 11–15 (1960).
8. Hohl, D. Cornified cell envelope. *Dermatologica* 180, 201–211 (1990).
9. Nguyen, V. T. *et al.* Programmed cell death of keratinocytes culminates in apoptotic secretion of a humectant upon secretagogue action of acetylcholine. *J. Cell Sci.* 114, 1189–1204 (2001).
10. Bikle, D. D., Xie, Z. & Tu, C. L. Calcium regulation of keratinocyte differentiation. *Expert Rev. Endocrinol. Metab.* 7, 461–472 (2012).
11. Kurasawa, M., Maeda, T., Oba, A., Yamamoto, T. & Sasaki, H. Tight junction regulates epidermal calcium ion gradient and differentiation. *Biochem. Biophys. Res. Commun.* 406, 506–511 (2011).
12. Hohl, D., Lichti, U., Breitkreutz, D., Steinert, P. M. & Roop, D. R. Transcription of the Human Loricrin Gene In Vitro Is Induced by Calcium and Cell Density and Suppressed by Retinoic Acid. *J. Invest. Dermatol.* 96, 414–418 (1991).
13. Burgeson, R. E. & Christianot, A. M. The dermal-epidermal junction. *Curr. Opin. Cell Biol.* 9, 651–658 (1997).
14. Breitkreutz, D., Koxholt, I., Thiemann, K. & Nischt, R. Skin basement membrane: the foundation of epidermal integrity-BM functions and diverse roles of bridging molecules nidogen and perlecan. *Biomed Res. Int.* 2013, 179784 (2013).
15. Kolarsick, P. A. J., Kolarsick, M. A. & Goodwin, C. Anatomy and Physiology of the Skin. *J. Dermatol. Nurses. Assoc.* 3, (2011).
16. Roger, M. *et al.* Bioengineering the microanatomy of human skin. *J. Anat.* 234, 438–455 (2019).
17. Ishikawa, H., Bischoff, R. & Holtzer, H. Mitosis and intermediate-sized filaments in developing skeletal muscle. 3, 538–555 (1968).
18. Szeverenyi, I. *et al.* The Human Intermediate Filament Database: comprehensive information on a gene family involved in many human diseases. *Hum. Mutat.* 29, 351–360 (2008).
19. Etienne-Manneville, S. Cytoplasmic Intermediate Filaments in Cell Biology. *Annu. Rev. Cell Dev. Biol.* 34, 1–28 (2018).
20. Moll, R., Divo, M. & Langbein, L. The human keratins: biology and pathology. *Histochem. Cell Biol.* 129, 705–733 (2008).
21. Moll, R., Franke, W. W., Schiller, D. L., Geiger, B. & Krepler, R. The catalog of human cytokeratins: patterns of expression in normal epithelia, tumors and cultured cells. *Cell* 31, 11–24 (1982).
22. Woodcock-Mitchell, J., Eichner, R., Nelson, W. G. & Sun, T. T. Immunolocalization of keratin polypeptides in human epidermis using monoclonal antibodies. *J. Cell Biol.* 95, 580–588 (1982).
23. Haines, R. L. & Lane, E. B. Keratins and disease at a glance. *J. Cell Sci.* 125, 3923–3928 (2012).
24. Kim, S. & Coulombe, P. A. Intermediate filament scaffolds fulfill mechanical, organizational,

and signaling functions in the cytoplasm. *Genes Dev.* 21, 1581–1597 (2007).
25. Jacob, J. T., Coulombe, P. A., Kwan, R. & Omary, M. B. Types I and II Keratin Intermediate Filaments. 10, 1–17 (2018).
26. Soellner, P., Quinlan, R. A. & Franke, W. W. Identification of a distinct soluble subunit of an intermediate filament protein: tetrameric vimentin from living cells. *Proc. Natl. Acad. Sci.* 82, 7929–7933 (1985).
27. Yoon, S. & Leube, R. E. Keratin intermediate filaments: intermediaries of epithelial cell migration. *Essays Biochem.* 63, 521–533 (2019).
28. Kouklis, P. D., Hutton, E. & Fuchs, E. Making a connection: direct binding between keratin intermediate filaments and desmosomal proteins. *J. Cell Biol.* 127, 1049–1060 (1994).
29. Wiche, G., Krepler, R., Artlieb, U., Pytela, R. & Aberer, W. Identification of plectin in different human cell types and immunolocalization at epithelial basal cell surface membranes. *Exp. Cell Res.* 155, 43–49 (1984).
30. Andrä, K. *et al.* Plectin-isoform-specific rescue of hemidesmosomal defects in plectin (-/-) keratinocytes. *J. Invest. Dermatol.* 120, 189–197 (2003).
31. Seltmann, K., Fritsch, A. W., Käs, J. A. & Magin, T. M. Keratins significantly contribute to cell stiffness and impact invasive behavior. *Proc. Natl. Acad. Sci. U. S. A.* 110, 18507–18512 (2013).
32. Coulombe, P. A., Kerns, M. L. & Fuchs, E. Epidermolysis bullosa simplex: a paradigm for disorders of tissue fragility. *J. Clin. Invest.* 119, 1784–1793 (2009).
33. Coulombe, P. A. *et al.* Point mutations in human keratin 14 genes of epidermolysis bullosa simplex patients: genetic and functional analyses. *Cell* 66, 1301–1311 (1991).
34. Liovic, M. *et al.* Severe keratin 5 and 14 mutations induce down-regulation of junction proteins in keratinocytes. *Exp. Cell Res.* 315, 2995–3003 (2009).
35. Ma, L., Yamada, S., Wirtz, D. & Coulombe, P. A. A 'hot-spot' mutation alters the mechanical properties of keratin filament networks. *Nat. Cell Biol.* 3, 503–506 (2001).
36. Breslin, S. & O'Driscoll, L. Three-dimensional cell culture: the missing link in drug discovery. *Drug Discov. Today* 18, 240–249 (2013).
37. Teimouri, A. 2D vs. 3D Cell Culture Models for In Vitro Topical (Dermatological) Medication Testing. in (ed. Yeung, P.) Ch. 1 (IntechOpen, 2019). doi:10.5772/intechopen.79868
38. Sun, T., Jackson, S., Haycock, J. W. & MacNeil, S. Culture of skin cells in 3D rather than 2D improves their ability to survive exposure to cytotoxic agents. *J. Biotechnol.* 122, 372–381 (2006).
39. Prunieras, M., Regnier, M. & Woodley, D. Methods for cultivation of keratinocytes with an air-liquid interface. *J. Invest. Dermatol.* 81, 28s-33s (1983).
40. Mak, V. H. W. *et al.* Barrier function of human keratinocyte cultures grown at the air-liquid interface. *J. Invest. Dermatol.* 96, 323–327 (1991).
41. Savini, I. *et al.* Characterization of keratinocyte differentiation induced by ascorbic acid: Protein kinase C involvement and vitamin C homeostasis. *J. Invest. Dermatol.* 118, 372–379 (2002).
42. Niehues, H. *et al.* Epidermal equivalents of filaggrin null keratinocytes do not show impaired skin barrier function. *J. Allergy Clin. Immunol.* 139, 1979-1981.e13 (2017).
43. Freeman, A. E., Igel, H. J., Herrman, B. J. & Kleinfeld, K. L. Growth and characterization of human skin epithelial cell cultures. *In Vitro* 12, 352–362 (1976).
44. Randall, M. J., Jüngel, A., Rimann, M. & Wuertz-Kozak, K. Advances in the Biofabrication of 3D Skin in vitro: Healthy and Pathological Models. *Front. Bioeng. Biotechnol.* 6, 154 (2018).
45. Klicks, J., von Molitor, E., Ertongur-Fauth, T., Rudolf, R. & Hafner, M. In vitro skin three-dimensional models and their applications. *J. Cell. Biotechnol.* 3, 21–39 (2017).
46. Alameda, J. P. *et al.* IKKα regulates the stratification and differentiation of the epidermis: implications for skin cancer development. *Oncotarget* 7, 76779–76792 (2016).
47. Moulin, V. *et al.* In vitro models to study wound healing fibroblasts. *Burn. , J. Int. Soc. Burn Inj.* 22, 359–362 (1996).
48. Hill, D. S. *et al.* A Novel Fully Humanized 3D Skin Equivalent to Model Early Melanoma Invasion. *Mol. Cancer Ther.* 14, 2665–2673 (2015).
49. Bataillon, M. *et al.* Characterization of a new reconstructed full thickness skin model, t-skin™, and its application for investigations of anti-aging compounds. *Int. J. Mol. Sci.* 20, (2019).
50. Frankart, A. *et al.* Epidermal morphogenesis during progressive in vitro 3D reconstruction at the

air-liquid interface. *Exp. Dermatol.* 21, 871–875 (2012).
51. Boukamp, P. *et al.* Normal Keratinization in a Spontaneously Immortalized Aneuploid Human Keratinocyte Cell Line. *J. Cell Biol.* 106, 761–771 (1988).
52. Boelsma, E., Verhoeven, M. C. H. & Ponec, M. Reconstruction of a human skin equivalent using a spontaneously transformed keratinocyte cell line (HaCaT). *J. Invest. Dermatol.* 112, 489–498 (1999).
53. Stark, H.-J., Szabowski, A., Fusenig, N. E. & Maas-Szabowski, N. Organotypic cocultures as skin equivalents: A complex and sophisticated in vitro system. *Biol. Proced. Online* 6, 55–60 (2004).
54. Maas-Szabowski, N., Stärker, A. & Fusenig, N. E. Epidermal tissue regeneration and stromal interaction in HaCaT cells is initiated by TGF-α. *J. Cell Sci.* 116, 2937–2948 (2003).
55. Berning, M., Prätzel-Wunder, S., Bickenbach, J. & Boukamp, P. Three-Dimensional In Vitro Skin and Skin Cancer Models Based on Human Fibroblast-Derived Matrix. *Tissue Eng. Part C. Methods* 21, 958–70 (2015).
56. Jung, M. H., Jung, S. M. & Shin, H. S. Co-stimulation of HaCaT keratinization with mechanical stress and air-exposure using a novel 3D culture device. *Sci. Rep.* 6, 1–7 (2016).
57. Choi, M. & Lee, C. Immortalization of primary keratinocytes and its application to skin research. *Biomol. Ther.* 23, 391–399 (2015).
58. Smits, J. P. H. *et al.* Immortalized N/TERT keratinocytes as an alternative cell source in 3D human epidermal models. *Sci. Rep.* 7, 1–14 (2017).
59. Reijnders, C. M. A. *et al.* Development of a Full-Thickness Human Skin Equivalent in Vitro Model Derived from TERT-Immortalized Keratinocytes and Fibroblasts. *Tissue Eng. - Part A* 21, 2448–2459 (2015).
60. Groeber, F., Holeiter, M., Hampel, M., Hinderer, S. & Schenke-Layland, K. Skin tissue engineering - In vivo and in vitro applications. *Adv. Drug Deliv. Rev.* 63, 352–366 (2011).
61. Bot, S. T. De, Willemsen, M. A. A. P., Vermeer, S. & Bot, S. T. De. Reviewing the genetic causes of spastic-ataxias. 79, 1507–14 (2012).
62. Espinós, C. Autosomal recessive cerebellar ataxias. 19, 1–19 (2006).
63. Bouhlal, Y., Amouri, R., Euch-fayeche, G. El & Hentati, F. Parkinsonism and Related Disorders Autosomal recessive spastic ataxia of Charlevoix e Saguenay : An overview. *Park. Relat. Disord.* 17, 418–422 (2011).
64. Berenznyakova, O. & Dupre, N. Spastic ataxias. in *Handbook of Clinical Neurology* (eds. Manto, M. & T.A.G.M, H.) 155, (Elsevier, 2018).
65. Fogel, B. L. & Perlman, S. Clinical features and molecular genetics of autosomal recessive cerebellar ataxias. *Lancet Neurol* 6, 245–57 (2007).
66. Synofzik, M. & Németh, A. H. Recessive ataxias. in *Handbook of Clinical Neurology* (eds. Subramony, S. H. & Dürr, A.) (Elsevier, 2018). doi:10.1016/B978-0-444-64189-2.00005-6
67. Vermeer, S., Brais, B. & Synofzik, M. ARSACS. *GeneReviews® [Internet]* 1–18 Available at: https://www.ncbi.nlm.nih.gov/books/NBK1255/.
68. Bouchard, J., Barbeau, A., Bouchard, R. & Bouchard, R. Autosomal Recessive Spastic Ataxia of Charlevoix-Saguenay. *Can. J. Neurol. Sci.* 5, 61–69 (1978).
69. Xiromerisiou, G. *et al.* A novel homozygous *SACS* mutation identified by whole exome sequencing-genotype phenotype correlations of all published cases. *J. Mol. Neurosci.* 70, 131–141 (2020).
70. Garcia-Martin, E. *et al.* Retinal segmentation as noninvasive technique to demonstrate hyperplasia in ataxia of Charlevoix-Saguenay. *Invest. Ophthalmol. Vis. Sci.* 54, 7137–42 (2013).
71. Synofzik, M., Soehn, A. S. & Gburek-Augustat, J. et al. Autosomal recessive spastic ataxia of Charlevoix Saguenay (ARSACS): Expanding the genetic, clinical and imaging spectrum. *Medizinische Genet.* 25, 137–138 (2013).
72. Ding, M., Weng, C., Fan, S., Cao, Q. & Lu, Z. Purkinje Cell Degeneration and Motor Coordination Deficits in a New Mouse Model of Autosomal Recessive Spastic Ataxia of Charlevoix-Saguenay. *Front. Mol. Neurosci.* 10, 121 (2017).
73. Bouchard, J.-P. *et al.* Autosomal recessive spastic ataxia of Charlevoix–Saguenay. *Neuromuscul. Disord.* 8, 474–479 (1998).
74. Stevens, J. C. *et al.* The ARSACS phenotype can include supranuclear gaze palsy and skin

lipofuscin deposits. *J. Neurol. Neurosurg. Psychiatry* 84, 114–116 (2013).
75. Cataldo, A. M., Hamilton, D. J. & Nixon, R. A. Lysosomal abnormalities in degenerating neurons link neuronal compromise to senile plaque development in Alzheimer disease. *Brain Res.* 640, 68–80 (1994).
76. Atanasova, S., Dimitrov, I., Kaprelyan, A. & Drenska, K. Gerstmann Syndrome in a Young Man: a Case Report. *Trakia J. Sci.* 16, 239–241 (2018).
77. Mrissa, N. *et al.* Linkage to chromosome 13q11-12 of an autosomal recessive cerebellar ataxia in a Tunisian family. *Neurology* 54, 1408–1414 (2000).
78. Breckpot, J. *et al.* A novel genomic disorder: A deletion of the *SACS* gene leading to Spastic Ataxia of Charlevoix-Saguenay. *Eur. J. Hum. Genet.* 16, 1050–1054 (2008).
79. Engert, J. C. *et al.* Autosomal recessive spastic ataxia of charlevoix-saguenay (ARSACS): High-resolution physical and transcript map of the candidate region in chromosome region 13q11. *Genomics* 62, 156–164 (1999).
80. Engert, J. C. *et al.* ARSACS, a spastic ataxia common in northeastern Quebec, is caused by mutations in a new gene encoding an 11.5-kb ORF. *Nat. Genet.* 24, 120–125 (2000).
81. Parfitt, D. A. *et al.* The ataxia protein sacsin is a functional co-chaperone that protects against polyglutamine-expanded ataxin-1. *Hum. Mol. Genet.* 18, 1556–1565 (2009).
82. Ouyang, Y. *et al.* Sacsin-related ataxia (ARSACS): Expanding the genotype upstream from the gigantic exon. *Neurology* 66, 1103 LP – 1104 (2006).
83. Takiyama, Y. Sacsinopathies: sacsin-related ataxia. *Cerebellum* 6, 353–359 (2007).
84. Gomez, C. M. ARSACS goes global. *Neurology* 62, 10–11 (2004).
85. Thiffault, I. *et al.* Diversity of ARSACS Mutations in French-Canadians. *Can. J. Neurol. Sci. / J. Can. des Sci. Neurol.* 40, 61–66 (2013).
86. Romano, A. *et al.* Comparative Analysis and Functional Mapping of *SACS* Mutations Reveal Novel Insights into Sacsin Repeated Architecture. *Hum. Mutat.* 34, 525–537 (2013).
87. Anderson, J. F., Siller, E. & Barral, J. M. The Sacsin Repeating Region (SRR): A Novel Hsp90-Related Supra-Domain Associated with Neurodegeneration. *J. Mol. Biol.* 400, 665–674 (2010).
88. Anderson, J. F., Siller, E. & Barral, J. M. The neurodegenerative-disease-related protein sacsin is a molecular chaperone. *J. Mol. Biol.* 411, 870–880 (2011).
89. Greer, P. L. *et al.* The Angelman Syndrome Protein Ube3A Regulates Synapse Development by Ubiquitinating Arc. *Cell* 140, 704–716 (2010).
90. Grynberg, M., Erlandsen, H. & Godzik, A. HEPN: a common domain in bacterial drug resistance and human neurodegenerative proteins. *Trends Biochem. Sci.* 28, 224—226 (2003).
91. Kozlov, G. *et al.* Structural basis of defects in the sacsin HEPN domain responsible for autosomal recessive spastic ataxia of Charlevoix-Saguenay (ARSACS). *J. Biol. Chem.* 286, 20407–20412 (2011).
92. Li, X. & Gehring, K. Structural studies of parkin and sacsin: Mitochondrial dynamics in neurodegenerative diseases. *Mov. Disord.* 30, 1610–1619 (2015).
93. Ménade, M. *et al.* Structures of ubiquitin-like (Ubl) and Hsp90-like domains of sacsin provide insight into pathological mutations. *J. Biol. Chem.* 293, 12832–12842 (2018).
94. Fagerberg, L. *et al.* Analysis of the human tissue-specific expression by genome-wide integration of transcriptomics and antibody-based proteomics. *Mol. Cell. Proteomics* 13, 397–406 (2014).
95. Uhlén, M. *et al.* Tissue-based map of the human proteome. *Science (80-.).* 347, 1260419 (2015).
96. Girard, M. *et al.* Mitochondrial dysfunction and Purkinje cell loss in autosomal recessive spastic ataxia of Charlevoix-Saguenay (ARSACS). *Proc. Natl. Acad. Sci. U. S. A.* 109, 1661–1666 (2012).
97. Criscuolo, C. *et al.* Powerhouse failure and oxidative damage in autosomal recessive spastic ataxia of Charlevoix-Saguenay. *J. Neurol.* 262, 2755–2763 (2015).
98. Tolkovsky, A. M. Mitophagy. *Biochim. Biophys. Acta - Mol. Cell Res.* 1793, 1508–1515 (2009).
99. Bradshaw, T. Y. *et al.* A reduction in Drp1-mediated fission compromises mitochondrial health in autosomal recessive spastic ataxia of Charlevoix Saguenay. *Hum. Mol. Genet.* 25, 3232–3244 (2016).
100. Smirnova, E., Griparic, L., Shurland, D.-L. & Van Der Bliek, A. M. Drp1 Is Required for Mitochondrial Division in Mammalian Cells. *Mol. Biol. Cell* 12, 2245–2256 (2001).
101. Morani, F. *et al.* Functional Transcriptome Analysis in ARSACS KO Cell Model Reveals a Role

of Sacsin in Autophagy. *Sci. Rep.* 9, 1–16 (2019).
102. Larivière, R. *et al.* Sacs knockout mice present pathophysiological defects underlying autosomal recessive spastic ataxia of Charlevoix-Saguenay. *Hum. Mol. Genet.* 24, 727–739 (2015).
103. Gentil, B. J. *et al.* Sacsin, mutated in the ataxia ARSACS, regulates intermediate filament assembly and dynamics. *FASEB J.* 33, 2982–2994 (2019).
104. Duncan, E. J. *et al.* Altered organization of the intermediate filament cytoskeleton and relocalization of proteostasis modulators in cells lacking the ataxia protein sacsin. *Hum. Mol. Genet.* 26, 3130–3143 (2017).
105. Dickson, M. A. *et al.* Human keratinocytes that express hTERT and also bypass a p16(INK4a)-enforced mechanism that limits life span become immortal yet retain normal growth and differentiation characteristics. *Mol. Cell. Biol.* 20, 1436–47 (2000).
106. Charest, J. L., Jennings, J. M., King, W. P., Kowalczyk, A. P. & García, A. J. Cadherin-mediated cell-cell contact regulates keratinocyte differentiation. *J. Invest. Dermatol.* 129, 564–572 (2009).
107. Bradford, M. M. A rapid and sensitive method for the quantitation of microgram quantities of protein utilizing the principle of protein-dye binding. *Anal. Biochem.* 72, 248–254 (1976).
108. Deyrieux, A. F., Rosas-Acosta, G., Ozbun, M. A. & Wilson, V. G. Sumoylation dynamics during keratinocyte differentiation. *J. Cell Sci.* 120, 125–136 (2007).
109. Seo, E.-Y. *et al.* Identification of calcium-induced genes in HaCaT keratinocytes by polymerase chain reaction-based subtractive hybridization. *Arch. Dermatol. Res.* 294, 411–418 (2002).
110. Waseem, A. *et al.* Keratin 15 Expression in Stratified Epithelia : Downregulation in Activated Keratinocytes. *J. Invest. Dermatol.* 112, 362–369 (1999).
111. Lyle, S. *et al.* The C8/144B monoclonal antibody recognizes cytokeratin 15 and defines the location of human hair follicle stem cells. *J. Cell Sci.* 111 (Pt 21), 3179–3188 (1998).
112. Bose, A., Teh, M.-T., Mackenzie, I. C. & Waseem, A. Keratin K15 as a biomarker of epidermal stem cells. *Int. J. Mol. Sci.* 14, 19385–19398 (2013).
113. Rice, R. H. & Green, H. Presence in human epidermal cells of a soluble protein precursor of the cross-linked envelope: activation of the cross-linking by calcium ions. *Cell* 18, 681–694 (1979).
114. Eckert, R. L. *et al.* Involucrin-structure and role in envelope assembly. *J. Invest. Dermatol.* 100, 613–617 (1993).
115. Drongelen, V. Van *et al.* Knock-down of filaggrin does not affect lipid organization and composition in stratum corneum of reconstructed human skin equivalents. *Exp. Dermatol.* 12, 807–812 (2013).
116. Drongelen, V. Van. Barrier Properties of an N/TERT-Based Human Skin Equivalent 1,2. 20, 3041–3049 (2014).
117. Wilson, V. G. Growth and differentiation of HaCaT keratinocytes. *Methods Mol. Biol.* 1195, 33–41 (2014).
118. Robinson, N. A., Lapic, S., Welter, J. F. & Eckert, R. L. S100A11, S100A10, Annexin I, Desmosomal Proteins, Small Proline-rich Proteins, Plasminogen Activator Inhibitor-2, and Involucrin Are Components of the Cornified Envelope of Cultured Human Epidermal Keratinocytes. *J. Biol. Chem.* 272, 12035–12046 (1997).
119. Aldehlawi, H. *et al.* Serum lipids, retinoic acid and phenol red differentially regulate expression of keratins K1, K10 and K2 in cultured keratinocytes. *Sci. Rep.* 10, 4829 (2020).
120. Krampert, M., Angelika, K., Braun, S. & Werner, S. Keratinocyte growth factor : effects on keratinocytes and mechanisms of action. 83, 607–612 (2004).
121. Marchese, C. *et al.* Human keratinocyte growth factor activity on proliferation and differentiation of human keratinocytes: Differentiation response distinguishes KGF from EGF family. *J. Cell. Physiol.* 144, 326–332 (1990).
122. Brady, S. P. Parakeratosis. *J. Am. Acad. Dermatol.* 50, 77–84 (2004).
123. Resnik, K. S. & DiLeonardo, M. Incidental Granular Parakeratotic Cornification in Carcinomas. *Am. J. Dermatopathol.* 29, 264–9 (2007).
124. Syrjänen, S., Mikola, H., Nykänen, M. & Hukkanen, V. In vitro establishment of lytic and nonproductive infection by herpes simplex virus type 1 in three-dimensional keratinocyte culture. *J. Virol.* 70, 6524–6528 (1996).
125. Schoop, V. M., Mirancea, N. & Fusenig, N. E. Epidermal organization and differentiation of HaCaT keratinocytes in organotypic coculture with human dermal fibroblasts. *J. Invest.*

Dermatol. 112, 343–353 (1999).
126. Breitkreutz, D. *et al.* Epidermal differentiation and basement membrane formation by HaCaT cells in surface transplants. *Eur. J. Cell Biol.* 75, 273–286 (1998).
127. Alloul-Ramdhani, M., Tensen, C. P. & El Ghalbzouri, A. Performance of the N/TERT epidermal model for skin sensitizer identification via Nrf2-Keap1-ARE pathway activation. *Toxicol. Vitr.* 28, 982–989 (2014).
128. Rheinwald, J. G. *et al.* A two-stage, p16(INK4A)- and p53-dependent keratinocyte senescence mechanism that limits replicative potential independent of telomere status. *Mol. Cell. Biol.* 22, 5157–5172 (2002).
129. Matsui, T. & Amagai, M. Dissecting the formation, structure and barrier function of the stratum corneum. *Int. Immunol.* 27, 269–280 (2015).
130. Ivanyi, D. *et al.* New monoclonal antibodies recognizing epidermal differentiation-associated keratins in formalin-fixed, paraffin-embedded tissue. Keratin 10 expression in carcinoma of the vulva. *J. Pathol.* 159, 7–12 (1989).
131. Murphy, G. F., Flynn, T. C., Rice, R. H. & Pinkus, G. S. Involucrin expression in normal and neoplastic human skin: a marker for keratinocyte differentiation. *J. Invest. Dermatol.* 82, 453–457 (1984).
132. Choi, K. H., Kim, G. M. & Kim, S. Y. The keratin-14 expression in actinic keratosis and squamous cell carcinoma: is this a prognostic factor for tumor progression? *Cancer Res. Treat.* 42, 107–114 (2010).
133. Alam, H., Sehgal, L., Kundu, S. T., Dalal, S. N. & Vaidya, M. M. Novel function of keratins 5 and 14 in proliferation and differentiation of stratified epithelial cells. *Mol. Biol. Cell* 22, 4068–4078 (2011).
134. Lloyd, C. *et al.* The basal keratin network of stratified squamous epithelia: defining K15 function in the absence of K14. *J. Cell Biol.* 129, 1329–1344 (1995).
135. Pontiggia, L. *et al.* Markers to Evaluate the Quality and Self-Renewing Potential of Engineered Human Skin Substitutes in vitro and after Transplantation. *J. Invest. Dermatol.* 129, 480–490 (2009).
136. Ponec, M., Boelsma, E., Gibbs, S. & Mommaas, M. Characterization of reconstructed skin models. *Skin Pharmacol. Appl. Skin Physiol.* 15 Suppl 1, 4–17 (2002).
137. UniProt: the universal protein knowledgebase in 2021. *Nucleic Acids Res.* 49, D480–D489 (2021).

8 Supplementary information

Table 8.1 Optimization of the HaCaT epidermal model. Different conditions (cell density, medium used in 2D culture prior to seeding on the insert, high calcium medium used on the submerged phase, air-liquid interface (ALI) conditions, number of ALI days) were tested to evaluate their influence morphology. EM- Epilife Medium.

Cells /cm^2 (x10^5)	2D Culture medium	High calcium medium	ALI conditions		Days of ALI
			medium	supplements	
2,50	DMEM	DMEM	DMEM	KGF+ Vit.C	12
5,00	DMEM	DMEM	DMEM	KGF+ Vit.C	12
8,33	DMEM	DMEM	DMEM	KGF+ Vit.C	20
2,50	EM 0,6mM Ca^{2+}	EM high Ca^{2+}	EM high Ca^{2+}	KGF+ Vit.C	12
5,00	EM 0,6mM Ca^{2+}	EM high Ca^{2+}	EM high Ca^{2+}	KGF+ Vit.C	14
5,00	EM 0,03mM Ca^{2+}	EM high Ca^{2+}	EM high Ca^{2+}	KGF+ Vit.C	14
5,83	EM 0,6mM Ca^{2+}	EM high Ca^{2+}	EM high Ca^{2+}	KGF+ Vit.C	12
5,83	EM 0,6mM Ca^{2+}	EM high Ca^{2+}	EM high Ca^{2+}	KGF+ Vit.C	14
5,83	EM 0,6mM Ca^{2+}	EM high Ca^{2+}	EM high Ca^{2+}	KGF+ Vit.C	16
5,83	EM 0,6mM Ca^{2+}	EM high Ca^{2+}	EM high Ca^{2+}	KGF+ Vit.C	18
5,83	EM 0,6mM Ca^{2+}	EM high Ca^{2+}	EM high Ca^{2+}	KGF+ Vit.C	21
5,83	EM 0,6mM Ca^{2+}	EM high Ca^{2+}	EM high Ca^{2+}	KGF+ Vit.C	23
5,83	EM 0,6mM Ca^{2+}	EM high Ca^{2+}	EM high Ca^{2+}	KGF+ Vit.C	26
5,83	EM 0,6mM Ca^{2+}	EM high Ca^{2+}	EM high Ca^{2+}	KGF+ Vit.C	28
5,83	EM 0,6mM Ca^{2+}	EM high Ca^{2+}	EM high Ca^{2+}	KGF+ Vit.C	31

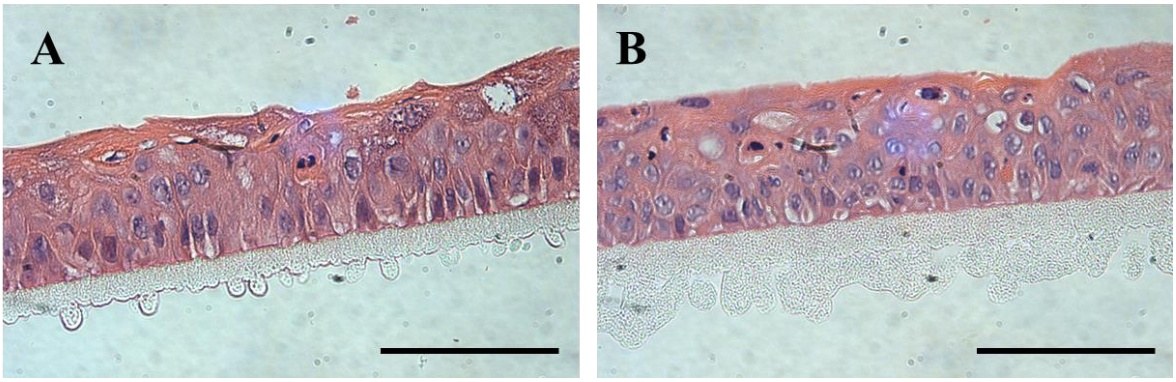

Figure 8.1 (A, B) Comparison of the effect of different calcium concentration prior to 3D culture in HaCaT epidermal morphology. Two different calcium concentrations were tested, 0,03mM (A) and 0,06mM (B). Same seeding cellular density ($5x10^5$ cells/cm^2) and the same number of air-liquid interface days (14) were used, both supplemented with L-ascorbic acid and keratinocyte growth factor (KGF). Reducing calcium concentration during cell culture (0,03mM) prior to seeding on the insert did not improve epidermal stratification, nor caused any significant morphological changes. Images were taken with a magnification of 400x. Scale bar is 100µm.

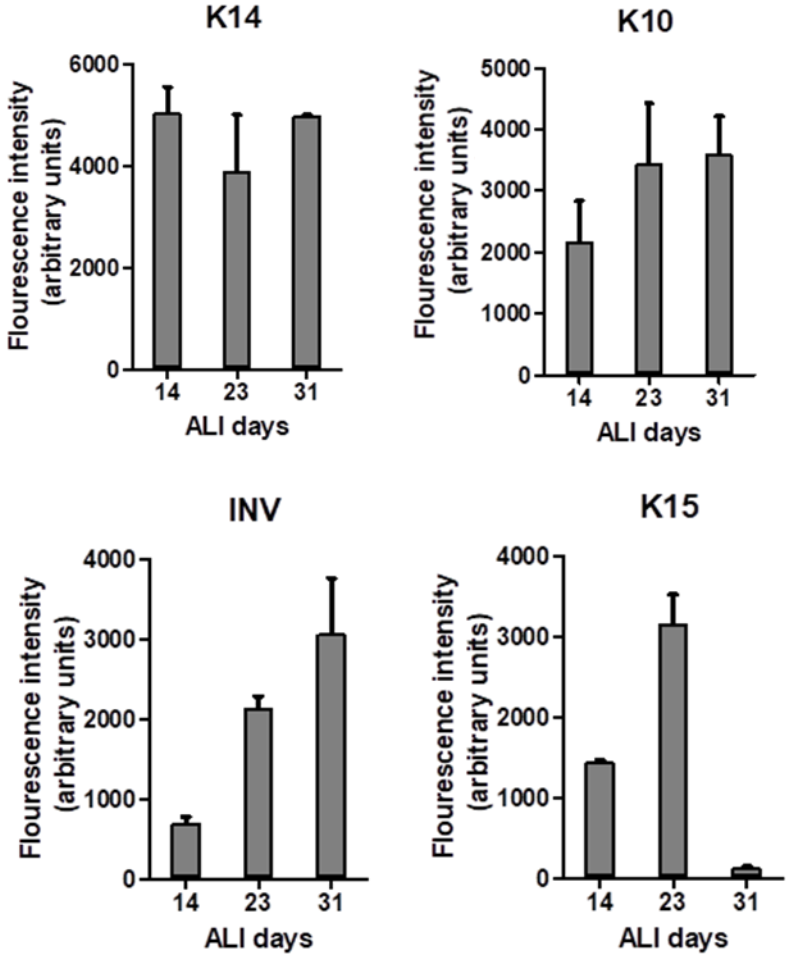

Figure 8.2 Fluorescence quantification of epidermal markers in the HaCaT cell model at different ALI days. The expression of keratin 14 (K14,), keratin 10 (K10), keratin 15 (K15) and involucrin (INV), were studied at 14, 23 and 31 ALI days. K14 expression showed similar levels from 14 to 31 ALI days. K10 expression had a higher expression after 23 ALI days, while INV showed an increase in expression with increasing ALI days, reaching its highest value after 31 ALI days. K15 expression increased from 14 to 23 ALI days, but after 31 ALI days showed low expression. These results were obtained from the images showed in Fig. 4.3, from only one independent experiment (2 were images measured per condition). Fluorescence intensity is shown in arbitrary units (Mean+SD)

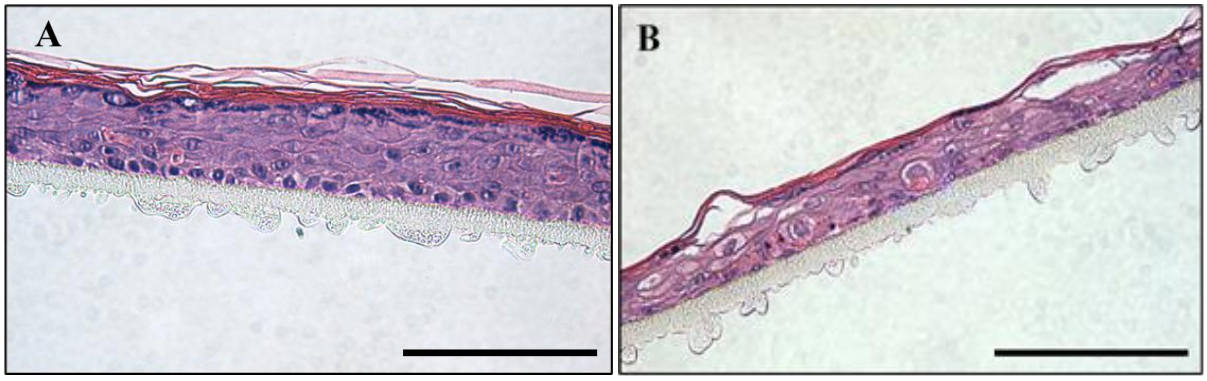

Figure 8.3 (A, B) Influence of cellular seeding density on improving morphology of the epidermal model using the N/TERT-1 cell line. Representative H&E stained images of the epidermal morphology with different cellular densities. Increasing cellular density to $5x10^5$cells/cm^2(A) did not improve stratification or thickness when compared to the conditions tested in Fig 3.4 A. Using a cellular density of $7.5x10^5$ cells/cm^2 resulted in a thinner epidermis with poor differentiated layers (B). Scale bar represents 100µm.